RAFAELA TEIXEIRA RODRIGUES DO VALE

FORMAÇÃO DE NANOCOMPLEXOS ENTRE β-LACTOGLOBULINA E RESVERATROL: UMA ABORDAGEM CINÉTICA E TERMODINÂMICA

Tese apresentada à Universidade Federal de Viçosa, como parte das exigências do Programa de Pós-Graduação em Ciência e Tecnologia de Alimentos, para obtenção do título de *Doctor Scientiae*.

Orientadora: Ana Clarissa dos Santos Pires

Coorientadores:
Luis Henrique Mendes da Silva
Márcia Cristina T. Ribeiro Vidigal

VIÇOSA - MINAS GERAIS
2022

Ficha catalográfica elaborada pela Biblioteca Central da Universidade Federal de Viçosa - Campus Viçosa

T
V149f
2022

Vale, Rafaela Teixeira Rodrigues do, 1990-
Formação de nanocomplexos entre β-lactoglobulina e resveratrol: uma abordagem cinética e termodinâmica / Rafaela Teixeira Rodrigues do Vale. – Viçosa, MG, 2022.
1 tese eletrônica (68 f.): il. (algumas color.).

Texto em português e inglês.
Orientador: Ana Clarissa dos Santos Pires.
Tese (doutorado) - Universidade Federal de Viçosa, Departamento de Tecnologia de Alimentos, 2022.
Inclui bibliografia.
DOI: https://doi.org/10.47328/ufvbbt.2022.681
Modo de acesso: World Wide Web.

1. Ligações químicas. 2. Proteínas. 3. Betalactoglobulina. 4. Resveratrol. 5. Ressonância. I. Pires, Ana Clarissa dos Santos, 1981-. II. Universidade Federal de Viçosa. Departamento de Tecnologia de Alimentos. Programa de Pós-Graduação em Ciência e Tecnologia de Alimentos. III. Título.

CDD 22. ed. 572.33

Bibliotecário(a) responsável: Euzébio Luiz Pinto CRB-6/3317

RAFAELA TEIXEIRA RODRIGUES DO VALE

FORMAÇÃO DE NANOCOMPLEXOS ENTRE β-LACTOGLOBULINA E RESVERATROL: UMA ABORDAGEM CINÉTICA E TERMODINÂMICA

Tese apresentada à Universidade Federal de Viçosa, como parte das exigências do Programa de Pós-Graduação em Ciência e Tecnologia de Alimentos, para obtenção do título de *Doctor Scientiae*.

APROVADA: 23 de agosto de 2022.

Assentimento:

Rafaela Teixeira Rodrigues do Vale
Autora

Ana Clarissa dos Santos Pires
Orientadora

À minha amada mamãe por todo o seu amor

AGRADECIMENTOS

A Deus, pelo dom da vida e por todas as oportunidades que contribuíram para o meu crescimento pessoal e profissional.

À Universidade Federal de Viçosa e ao Programa de Pós-Graduação em Ciência e Tecnologia de Alimentos, pela oportunidade de realizar a pós-graduação.

À Coordenação de Aperfeiçoamento de Pessoal de Nível Superior (CAPES), pela concessão da bolsa de estudos. Ao Conselho Nacional de Desenvolvimento Científico e Tecnológico (CNPq), a Fundação de Apoio à Pesquisa de Minas Gerais (FAPEMIG) e Financiadora de Estudos e Projetos (FINEP) pelo suporte financeiro. O presente trabalho foi realizado com apoio da CAPES – Brasil – Código de Financiamento 001.

À minha família, em especial a minha amada mamãe Edna e ao José Marcos pelo carinho, apoio e amor incondicional. A minha irmã Juliana por sua constante presença e por ter me presenteado com o quarteto fantástico (Manuela, Yasmim, Tales e Isabela). Crianças, vocês tornam os meus dias mais felizes e muito me ensinam sobre o amor na sua mais perfeita pureza.

Às minhas Tias Eliane Rodrigues, Eliane Teixeira, Maria de Fátima e Rita, por todo carinho e orações. Agradeço em especial, ao meu Tio Valdinei Carlos que nos meses antecedentes a conclusão deste trabalho, me acompanhou durante o meu tratamento médico. Sem sombras de dúvidas, a sua presença durante cada procedimento, me trouxeram e trazem segurança, serenidade, paz e a constante esperança por dias melhores. Obrigada por tanto! Você é benção em nossas vidas!

À professora Ana Clarissa, pela acolhida, orientação, ensinamentos e compreensão nos momentos adversos.

Aos meus coorientadores Luis Henrique e Márcia Cristina, pela disponibilidade, parceria e conhecimentos compartilhados.

Aos membros da banca do exame de qualificação (Professoras Ana Clarissa, Márcia Cristina, Jaqueline Rezende, Yara Coelho e Professor Luis Henrique), por aceitarem participar deste trabalho e pelas importantes sugestões para a sua composição.

Aos egressos e ingressos do grupo THERMA. A cada um de vocês, minha gratidão pelo convívio profissional e pelos ensinamentos compartilhamento ao longo de todos os treinamentos. Agradeço especialmente a Nayara e a Lívia, pelo estímulo

e encorajamento para superar as adversidades inerentes à realização deste trabalho.

Ao grupo QUIVECOM, pela parceria, disponibilidade de equipamentos, dados e reagentes.

Aos meus amigos acadêmicos e não acadêmicos, pela escuta empática, incentivo e sobretudo, pela rede de apoio nos momentos mais desafiadores. Carinhosamente, agradeço a Alan Coutinho, Ana Flávia, Bruno Moreno, Carini Lelis, Daniel Rodrigues, Débora Adinair, Jeíce, Josiana, Luciana, Lucidarce, Louani, Paulo Henrique, Regiane Marcolino e Roney. Vocês são presentes de Deus em minha vida.

“Conheça todas as teorias, domine todas as técnicas, mas ao tocar uma alma humana, seja apenas outra alma humana”.

(Carl Jung)

RESUMO

VALE, Rafaela Teixeira Rodrigues do, D.Sc., Universidade Federal de Viçosa, agosto de 2022. **Formação de nanocomplexos entre β-lactoglobulina e resveratrol: uma abordagem cinética e termodinâmica**. Orientadora: Ana Clarissa dos Santos Pires. Coorientadores: Luis Henrique Mendes da Silva e Márcia Cristina Teixeira Ribeiro Vidigal.

O estudo da cinética e da termodinâmica de interação intermolecular entre moléculas de origem alimentar fornece a dinâmica de formação de nanocomplexos, bem como, a compreensão das forças motrizes envolvidas neste processo. A β-lactoglobulina (βLG), proteína majoritária do soro de leite de muitos mamíferos, além de características nutricionais relevantes, apresenta capacidade de se ligar a pequenos compostos bioativos hidrofóbicos como o resveratrol (RES) e de formar nanocomplexos de βLG-RES. No entanto, embora alguns estudos tratem da interação entre estas duas moléculas, há uma lacuna em relação a dinâmica de formação destes nanocomplexos. Em nosso trabalho, utilizando a técnica de ressonância plasmônica de superfície (SPR), determinamos os parâmetros cinéticos e termodinâmicos da interação βLG-RES. Os resultados mostraram que a formação do complexo ativado a partir da associação de moléculas livres é 1,5 vezes mais rápida do que a partir da dissociação do complexo termodinamicamente estável ($\Delta G^{\ddagger}_{(a)} \cong$ 48,15 kJ.mol^{-1}, $\Delta G^{\ddagger}_{(d)} \cong$ 73,10 kJ.mol^{-1}). Além disso, os parâmetros cinéticos de associação são influenciados pela estrutura 3D da água da camada de solvatação de ambas moléculas. Entretanto, os parâmetros cinéticos de dissociação não são influenciados pelas moléculas de água presentes ao redor do complexo termodinamicamente estável. Provavelmente, porque há poucas moléculas de água próxima/dentro do sítio de interação da proteína. Ademais, as moléculas de água que estão presentes, não estão estruturadas. Os valores negativos de $\Delta G°$ (-24,95 KJ.mol^{-1}) indicaram que, no equilíbrio químico, o complexo termodinamicamente estável predomina sobre as moléculas livres. Na menor temperatura (285,15K) avaliada, a formação do complexo βLG-RES foi impulsionada por interações hidrofóbica ($\Delta H°$ = 73.06 kJ.mol^{-1}; $T\Delta S°$ = 99.60 kJ.mol^{-1}) enquanto que em temperaturas maiores que 301,15K, as interações hidrofílicas tornaram-se dominantes ($\Delta H°$ = -142,50 kJ.mol^{-1}; $T\Delta S°$ = -118,18 kJ.mol^{-1}). Contudo, a partir destes resultados, apresentamos valiosas informações e insights para a

compreensão da dinâmica molecular de formação de nanocomplexos βLG-RES e, das forças motrizes que impulsionam este processo.

Palavras-chave: Interação intermolecular. Proteína. Polifenol. Nanocarreador.

ABSTRACT

VALE, Rafaela Teixeira Rodrigues do, D.Sc., Universidade Federal de Viçosa, August, 2022. **Nanocomplex formation between β-lactoglobulin and resveratrol: a kinetics and a thermodynamics approach**. Adviser: Ana Clarissa dos Santos Pires. Co-advisers: Luis Henrique Mendes da Silva and Márcia Cristina Teixeira Ribeiro Vidigal.

The study of the kinetics and thermodynamics of the intermolecular interaction between molecules of food origin provides the dynamics of the formation of nanocomplexes, as well as the understanding of the driving forces involved in this process. β-lactoglobulin (βLG), the major whey protein of many mammals, in addition to relevant nutritional characteristics, has the ability to bind small hydrophobic bioactive compounds such as resveratrol (RES) and to form βLG-RES nanocomplexes. However, although some studies deal with the interaction between these two molecules, there is a gap regarding the dynamics of formation of these nanocomplexes. In our work, using the surface plasmon resonance (SPR) technique, we determined the kinetic and thermodynamic parameters of the βLG-RES interaction. The results showed that the formation of complex activated by the association of free molecules is 1.5 times faster than from the dissociation of the thermodynamically stable complex ($\Delta G^{\ddagger}_{(a)} \cong$ 48.15 kJ.mol^{-1}, $\Delta G^{\ddagger}_{(d)} \cong$ 73.10 kJ.mol^{-1}). Furthermore, the association kinetic parameters are influenced by the 3D water structure of the solvation layer of both molecules. However, the kinetic parameters of dissociation are not influenced by the water molecules present around the thermodynamically stable complex. Probably because there are few water molecules near/inside the protein interaction site. Furthermore, the water molecules that are present are not structured. The negative values of ΔG° (-24.95 KJ.mol^{-1}) indicated that, in chemical equilibrium, the thermodynamically stable complex predominates over the free molecules. At the lowest temperature (285.15K) evaluated, the formation of the βLG-RES complex was driven by the hydrophobic interaction (ΔH° = 73.06 kJ.mol^{-1}; TΔS° = 99.60 kJ.mol^{-1}) while at temperatures greater than 301.15K, hydrophilic interactions became dominant (ΔH° = -142.50 kJ.mol^{-1}; TΔS° = -118.18 kJ.mol^{-1}). However, from these results, we present valuable information and insights for understanding the molecular dynamics of βLG-RES nanocomplex formation and the driving forces that drive this process.

Keywords: Intermolecular interaction. Protein. Polyphenol. Nanocarrier.

LISTA DE FIGURAS

CAPÍTULO 1 – REVISÃO DE LITERATURA

CAPÍTULO 2: β-LACTOGLOBULIN AND RESVERATROL NANOCOMPLEX FORMATION IS DRIVEN BY SOLVATION WATER RELEASE

LISTA DE SIGLAS E ABREVIATURAS

αLA - α-lactoalbumina

βLG - β-lactoglobulina

BSA - Albumina do soro bovino

HSA - Albumina do soro humano

LG - Imunoglobulina

RES - Resveratrol

EGCG - Epigalocatequina-3-galato

SPR - Ressonância plasmônica de superfície

Trp - Triptofano

Tyr – Tirosina

Cys - Cisteína

Phe - Fenilalanina

RU - Resposta ressonante

K_b - Constante de interação

k_a - Constante cinética de associação

k_d - Constante cinética de dissociação

n - Estequiometria

ΔG° - Variação da energia livre de Gibbs padrão de formação de complexo

ΔS° - Variação da entropia padrão de formação de complexo

ΔH° - Variação da entalpia padrão de formação de complexo

$E_{ativ(a)}$ - Energia de ativação relacionada a associação de moléculas livres

$E_{ativ(d)}$ – Energia de ativação relacionada a dissociação do complexo termodinamicamente estável

$\Delta H^{‡}_{(a)}$ - Variação da entalpia de ativação de associação

$\Delta H^{‡}_{(d)}$ - Variação da entalpia de ativação de dissociação

$\Delta G^{‡}_{(a)}$ - Variação da energia livre de Gibbs de ativação de associação

$\Delta G^{‡}_{(d)}$ - Variação da energia livre de Gibbs de ativação de dissociação

$\Delta S^{‡}_{(a)}$ - Variação da entropia de ativação de associação

$\Delta S^{‡}_{(d)}$ - Variação da entropia de ativação de dissociação

SUMÁRIO

INTRODUÇÃO GERAL

A β-lactoglobulina (βLG), uma das principais proteínas da fração do soro do leite de muitos mamíferos, incluindo, entre outros, a família *Bovidae*, apresenta estrutura bem definida, mas, que pode sofrer alterações em virtude de fatores externos como temperatura e pH. Dependendo das condições do meio, esta proteína apresenta a capacidade de interagir fortemente com pequenos compostos hidrofóbicos e, de transportar inúmeras moléculas, incluindo uma variedade de fármacos e de compostos alimentares como aromáticos, vitamínicos e antioxidantes como o resveratrol.

O resveratrol (RES) é um exemplo de polifenol que tem despertado grande interesse na comunidade acadêmica e, que pode ser obtido naturalmente a partir de mais de 70 plantas, de diferentes frutas (uva, mirtilo, framboesa e amora) e, de alimentos processados como vinho tinto e chocolate amargo.

Este composto bioativo tem sido relacionado a propriedades funcionais como antioxidantes, anti-inflamatórias, neuro e cardioprotetoras, anticarcinogênicas, antienvelhecimento, antidiabética e antiobesidade. Além disso, considerando sua característica hidrofóbica, diferentes estudos apontam a sua capacidade de interação com a βLG e, consequentemente, de proteger estes compostos contra alguns fatores comumente aplicados durante o processamento e a estocagem de alimentos (variações de temperatura, pH e luminosidade). Entretanto, embora este tipo de interação já tenha sido relatada por alguns pesquisadores, a literatura carece de informações completas sobre a termodinâmica de interação entre estas duas moléculas. Além disso, dados sobre a cinética de formação de complexo βLG-RES não estavam disponíveis. Estas informações são fundamentais para a utilização de proteínas como nanocarreadores viáveis para moléculas bioativas.

A ressonância plasmônica de superfície (SPR) é uma técnica que em tempo real, permite que em um único experimento, se possa obter dados a respeito da interação intermolecular entre as moléculas responsáveis pela formação de complexo βLG-RES.

Assim, visando traçar o perfil da dinâmica de interação entre βLG e RES e, fornecer novos *insights* sobre o assunto, este trabalho está dividido em dois capítulos. O Capítulo 1 consiste em uma revisão bibliográfica geral sobre cada uma

das moléculas envolvidas na interação assim como, sobre a técnica de SPR. Na sequência, na forma de artigo científico, o Capítulo 2 apresenta os resultado da cinética e da termodinâmica da formação de complexo entre a proteína e o composto bioativo.

CAPÍTULO 1: Revisão de literatura

1. β-lactoglobulina (βLG)

O leite bovino é um importante fluido biológico que em média, apresenta 87,3% (m/v) de água e 12,7% de sólidos totais, dos quais 3,5% correspondem às proteínas. Deste total de conteúdo proteico, cerca de 80% são de caseínas (αs1-, αs2-, β- e κ-caseína com razão molar de aproximadamente 3:1:3:1, respectivamente) e, os outros 20% das chamadas proteínas do soro de leite (53,6% (m/v) de β-lactoglobulina (βLG), 20,1% (m/v) de α-lactoalbumina (αLA), 6,2% (m/v) de albumina do soro bovino (BSA), 3,5% de imunoglobulinas (LG), dentre outras) (Hailu et al., 2016; Lajnaf et al., 2022).

A βLG é uma proteína globular com ponto isoelétrico em pH de aproximadamente 5,1, massa molar de 18,3 kDa e 162 resíduos de aminoácidos dos quais cinco são de cisteína e quatro deles formam pontes dissulfeto. Em sua forma nativa, a βLG é predominantemente formada por estruturas secundárias do tipo β-folha, contendo oito fitas β, e uma α-hélice (Brownlow et al., 1997; Kurpiewska et al., 2019; Olsen et al., 2022), Figura 1.

Figura 1 – Representação da β-lactoglobulina na forma nativa. Imagem criada com o ID do PDB e visualizador NGL.

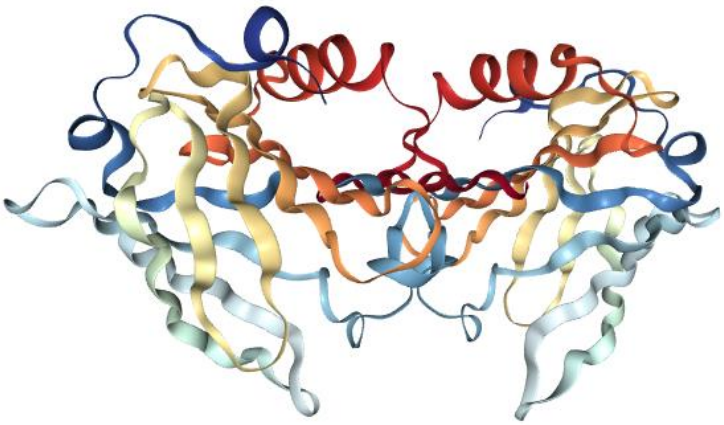

Fonte: http://www.rcsb.org/3d-view/2Q2M/1

Geneticamente, a βLG apresenta diferentes variantes. Entre as mais abundantes, destacamos as variantes A e B que se diferem entre si pela presença

de resíduos de aminoácidos nas posições 64 (Asp64 e Gly64 nas variantes A e B, respectivamente) e 118 (Val118 e Ala118 nas variantes A e B, respectivamente). Estas diferenças tornam as duas variantes ligeiramente diferentes em relação às propriedades de auto associação, à solubilidade, ao ponto isoelétrico, bem como, a estabilidade à pressão e à temperatura. No caso específico da βLG bovina, as características estruturais das variantes A e B são praticamente indistinguíveis (Taulier & Chalikian, 2001).

No estado nativo, a βLG apresenta núcleo formado por um barril β achatado (um cálice) composto por oito cadeias antiparalelas (A a H). Alterações de pH podem induzir transições estruturais locais e globais na molécula proteica (Wang et al., 2021). Abaixo do pH 3, o dímero se dissocia em monômeros que preservam sua conformação nativa. Próximo ao pH 3, a proteína dimeriza com poucas alterações na estrutura. Entre o pH 4 e o pH 5, ocorre a transição de dímero para octâmero e estudos mostram que a octamerização da proteína não causa mudança em sua estrutura secundária. Entre o pH 4,5 e pH 6,0 a βLG é convertida da sua forma Q ácida expandida para a forma N nativa mais compacta. Essa transição envolve mudanças na estrutura e hidratação da proteína. Acima do pH 6,5, a molécula sofre a chamada transição de Tanford que consiste na mudança reversível de conformação de um dos laços que circundam a entrada do barril β e que é desencadeada pela protonação de Glu 89 e elevação do valor do pK_a (Świątek et al., 2019; Taulier & Chalikian, 2001).

A transição de Tanford envolve o deslocamento da alça EF (resíduos 85 a 90) que atua como uma tampa que fecha o interior da proteína/local de ligação abaixo de pH 7,3 e a abre em pH mais alto. A transição de Tanford também pode envolver outras mudanças estruturais (Zhu et al., 2020). Por exemplo, a transição é acompanhada por uma mudança no microambiente de Tyr42 e causa uma alteração na orientação relativa dos monômeros no dímero em até 5°. Em pH maiores que 9, a βLG sofre uma transição de desdobramento irreversível, induzida pela base, com ruptura global de estruturas secundárias e terciárias (Vijayalakshmi et al., 2008).

Embora ainda se tenha dúvidas da real função da βLG no organismo, as informações a respeito da conformação, estrutura tridimensional bem como, de suas propriedades físico-químicas já se encontram bem consolidadas. Essa proteína é responsável não apenas pela captação, mas, pelo transporte de moléculas

hidrofóbicas. Trata-se de um modelo útil para o estudo de interações proteína-ligante (Muresan et al., 2001; Wang et al., 2021; Zhang et al., 2022).

Na literatura, vários compostos têm sido relatados como ligantes da βLG. Dentre eles podemos citar: retinol e lactona (Muresan et al., 2001), ácido láurico (Bello et al., 2012), fármacos como amoxicilina (Habibian-Dehkordi et al., 2022), doxorrubicina (Ghalandari et al., 2014), tetracaína e promacaína (Loch et al., 2015), carotenoide como licopeno (Dima et al., 2018) e antioxidantes como epigalocatequina-3-galato (EGCG) (Zagury et al., 2019) e o resveratrol (Cheng et al., 2018; Guo & Jauregi, 2018; Liang & Subirade, 2012; Liang et al., 2008; Wusigale et al., 2017; Zhang et al., 2022; Vale et al., 2022).

Guo e Jauregi (2018), avaliaram a atividade antioxidante do RES (7 mg/100 mL) na forma livre e complexado com a βLG (nativa e nanoparticulada). Quando livre e considerando o método de atividade antioxidante total, a capacidade antioxidante (% de inibição) do polifenol reduziu. Por outro lado, quando na presença da proteina, a capacidade antioxidante aumentou em aproximadamente 20 e 22,5% para βLG na forma nativa e nanopartículas, respectivamente.

Recentemente, Zhang et al. (2022), utilizando abordagens multiespectroscópicas, docking molecular e simulação de dinâmica molecular, avaliaram a interação isolada e simultânea do RES e da curcumina (CUR) com a βLG. Os espectros de fluorescência, infravermelho com transformada de Fourier (FT-IR), CD, difração de raios X (XRD) e, de calorimetria diferencial de varredura (DSC) indicaram que o RES e a CUR interagem individualmente e simultaneamente com a βLG. Para a termodinâmica de interação, os autores apenas calcularam os valores da constante de ligação (K_b) e da estequiometria (n) que foram 1,86 × 10^6 M^{-1} e 1,33 ± 0,02, respectivamente. Os demais parâmetros termodinâmicos, não foram avaliados. A interação do RES com a βLG melhorou a atividade antioxidante do RES e reforça a capacidade da proteína em proteger o polifenol.

Assim, o estudo aprofundado sobre a interação entre a βLG e o resveratrol (RES), trata de um avanço dentro da área de interação intermolecular e, que é capaz de fornecer informações a respeito do carreamento deste polifenol pela proteína de transporte.

2. Resveratrol (RES)

O resveratrol (3,5,4′-trihidroxiestilbeno) é uma fitoalexina natural que foi isolada pela primeira vez no ano de 1940 a partir das raízes do heléboro branco (*Veratrum grandiflorum O.* Loes). Já em 1963, o resveratrol (RES) começou a ser extraído de raízes da *Polygonum cuspidatum*, planta utilizada na Medicina Tradicional Chinesa (Huang et al., 2019).

Atualmente, sabe-se que o RES pode ser obtido extraído de mais de 70 outras plantas e, através de produtos processados (vinho tinto e chocolate amargo), bem como, de alimentos naturais como uva, mirtilo, framboesa, amora, dentre outros (Burns et al., 2002; Lin et al., 2016).

Em termos de estrutura química, o RES é um polifenol natural com estrutura de estilbeno, composta por dois anéis aromáticos interligados por uma ponte de etileno e, duas formas isoméricas (*trans* e *cis*), Figura 2.

Figura 2 - Estrutura química do *trans*-resveratrol (A) e do *cis*-resveratrol (B).

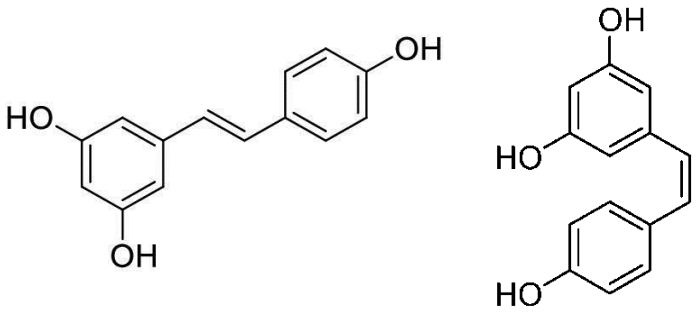

(A) **(B)**

Fonte: Autora, 2021.

É considerado um dos estilbenos mais amplamente investigado por sua bioatividade e possíveis aplicações terapêuticas, incluindo: anti-inflamatória, antioxidante, anticancerígena, antiobesidade, antienvelhecimento, cardioprotetora, neuroprotetora e de regulação da homeostase da glicose (Chen et al., 2019).

Apresenta fórmula molecular $C_{14}H_{12}O_3$, massa molar de 228,247 g mol^{-1}, ponto de fusão entre 253 e 255 °C (Amri et al., 2012), três constantes de dissociação ácidas ($pK_{a1,2,3}$ = 8,8, 9,8 e 11,4) provenientes da desprotonação dos grupos hidroxilas presentes no composto (López-Nicolás & García-Carmona, 2008), coeficiente de partição igual a 3,1 (Robinson et al., 2015), baixa solubilidade em

água (0,023 mg ml^{-1} a 25 ˚C) e considerável solubilidade em etanol (50 mg ml^{-1} a 25 ˚C) e DMSO (16 mg ml^{-1} a 25 ˚C) (Fan et al., 2018).

No geral, a administração do RES é dificultada pelas restrições relacionadas a sua solubilização em solventes aquosos, curto tempo de meia-vida *in vivo* (cerca de 8 a 14 minutos), baixa biodisponibilidade oral e alta instabilidade química em meios aquosos (tendência a sofrer oxidação e alta fotossensibilidade) (Santos et al., 2019). Nesse contexto, estudos têm sido desenvolvidos com o objetivo de projetar novas perspectivas de utilização deste polifenol.

O RES apresenta capacidade de formar complexos com diferentes proteínas como as proteínas de ervilhas (Yi et al., 2022), zeinas (Liang et al., 2018; Liu et al., 2022), glutelina de arroz (Dai et al., 2019), isolado de proteínas de soja (Pujara et al., 2017), isolado de proteina de soro de leite (Xu et al., 2021), β-caseína (Cheng et al., 2020), albumina do soro humano (HSA) (Cao et al., 2009; Jiang, 2008; N′ soukpoé-Kossi et al., 2006; Nair, 2015; Pantusa et al., 2012; Poór et al., 2022; Rezende et al., 2020), BSA (Arcanjo et al., 2018; Bourassa et al., 2010; Lu et al., 2007), αLA (Cheng et al., 2018) e βLG (Cheng et al., 2018; Guo & Jauregi, 2018; Liang & Subirade, 2012; Liang et al., 2008; Ojaghian et al., 2016; Wusigale et al., 2017; Zhang et al., 2022).

Para o caso específico da interação entre o RES e a βLG, a literatura carece de informações completas a respeito da termodinâmica de interação. Os dados disponíveis na literatura apenas se referem aos valores da constante de ligação e da estequiometria relacionada com a quantidade de moléculas de RES que interagem em cada sítio de ligação da βLG. Até a construção dos objetivos deste trabalho, não haviam dados sobre a variação da energia livre de Gibbs ($\Delta G°$), da entropia ($T\Delta S°$) e entalpia ($\Delta H°$) padrão de formação de complexo βLG-RES. A interação apenas havia sido avaliada por meio de abordagens multiespectroscópicas, docking molecular e simulação de dinâmica molecular. Não haviam informações sobre a cinética de formação do complexo. Dados sobre a taxa de associação das moléculas que interagem para formar complexo e, sobre a taxa de dissociação do complexo ainda eram desconhecidos. Além disso, para a interação entre estas moléculas, a técnica de ressonância plasmônica de superfície ainda não havia sido utilizada.

3. Ressonância Plasmônica de Superfície (SPR)

A Ressonância Plasmônica de Superfície (SPR) trata-se de uma técnica óptica capaz de fornecer com alta sensibilidade, confiabilidade, seletividade, reprodutibilidade e desempenho qualitativo/quantitativo (Jebelli et al., 2020), os parâmetros cinéticos e termodinâmicos envolvidos na interação intermolecular entre proteína (βLG) e analito (RES) (Nunes et al., 2019).

3.1 Princípio geral do SPR

Em sistemas baseados em SPR, tem-se a presença de um *chip* sensor que para estudo de interação, utiliza-se por exemplo, o CM5 que é constituído por uma camada de vidro, uma camada de ouro e uma camada de carboximetildextrana (local onde a proteína alvo do estudo deverá ser imobilizada). Assim, neste tipo de experimento, inicialmente deve-se proceder com a ativação do *chip*, imobilização da proteína (βLG) e bloqueio dos grupos funcionais restantes que não estão interagindo com a molécula proteica. Na sequência, um fóton de luz incidente atinge a superfície do c*hip* de forma que a maior parte desta radiação é refletida e uma pequena parte (menos de 0,01% da radiação de origem, chamada radiação evanescente) é refratada em aproximadamente 100 nm acima da camada de ouro. Ao retornar, a radiação refratada volta com determinado ângulo θ (chamado θ_1) e faz com que os elétrons livres na superfície da camada de ouro entrem em ressonância plasmônica (vibrem na mesma frequência). Este ângulo θ é dependente do índice de refração e da composição da solução acima da superfície da camada de ouro do *chip* sensor. Logo, quando se injeta a solução contendo o analito e, quando ele interage com proteína, o índice de refração desta solução é alterado e consequentemente, tem-se um novo ângulo θ (chamado de θ_2). A diferença entre os ângulos θ_1 e θ_2 fornece a resposta ressonante (RU), que é plotada em função do tempo. A variação de RU versus tempo é chamada de sensograma (Nguyen et al., 2015; Vachali et al., 2015). Através dos sensogramas e conforme será discutido no tópico 3.4, a dinâmica de formação de nanocomplexos é determinada.

3.2 Equipamentos

A tecnologia de biossensor baseada no fenômeno óptico SPR foi introduzida nos anos 90 especialmente, pela BiacoreTM (marca registrada da GE Healthcare) que atualmente, conta com diferentes equipamentos (Biacore™ X, Biacore™ X100,

Biacore™ 2000, Biacore™ 3000, Biacore™ T200, Biacore™ 8 e Biacore™ 8+) de sensibilidade e especificidade distintas. Esses equipamentos são compostos principalmente por três componentes básicos: sistema de medição óptica, sistema de manuseio de fluido e chip sensor (Katsamba et al., 2002; Nguyen et al., 2015; Situ et al., 2010).

Além da BiacoreTM, existem outras marcas que são úteis e eficientes para o diagnóstico médico (Gade et al., 2022), triagem de medicamentos (Chain et al., 2021), proteção ambiental (Zhang et al., 2021), detecção de adulteração em alimentos (Mansouri et al., 2020; Vikas et al., 2020), detecção de resíduos de antibióticos em alimentos (Ramalingam et al., 2021).

No geral, para o estudo de interação intermolecular entre componentes alimentares, os instrumentos de SPR são baseados em biossensores do tipo prisma e que podem operar de acordo com as configurações Otto e Kretschmann (Ravindran et al., 2021).

Biossensores com configuração Otto são considerados de difícil fabricação e uso uma vez que, apresentam estrutura de acoplamento composta por um filme metálico de alto índice de refração e, presença de gap para a célula de amostra, Figura 3 (A). Por outro lado, os prismas de configuração Kretschmann (Figura 3 (B)), não possuem gap para a célula de amostra. Neste caso, a célula de amostra fica diretamente sob o filme metálico e assim, facilita o controle de parâmetros e variáveis que influenciam na análise. Logo, no que se refere a biossensores do tipo prisma, a configuração de Kretchmann é a mais utilizada e caracterizada como uma técnica padrão (Yesudasu et al., 2021; Zhou et al., 2019).

Figura 3 - Tipos de configurações de SPR: (A) Otto (B) Kretschmann.

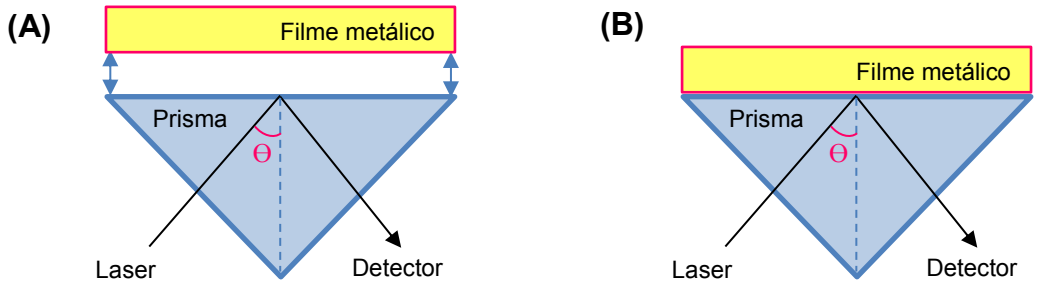

Fonte: Autora, 2021.

3.3 Imobilização da proteína

Considerando aplicações específicas de SPR para análise de interações proteínas-bioativos, parte-se do princípio que as moléculas proteicas estão imobilizadas na superfície do chip sensor e as bioativas, livres em solução (Rezende et al., 2020).

Assim, o mercado mundial conta com uma grande variedade de chips sensores que podem ser selecionados de acordo com a química de superfície necessária para a ocorrência da imobilização da proteína. Um dos chips mais popularmente utilizado é o carboximetil-dextrano (chamado de CM5) que contém grupo carboxila e dois canais de fluxo: o canal de amostra (onde a proteína será imobilizada) e o canal de controle (Schneider et al., 2015).

A imobilização da proteína à superfície do chip pode ser realizada por meio de acoplamento covalente que para estudos de interação é o método de imobilização mais comumente utilizado e caracterizado pela ligação química do grupo funcional da proteína, neste caso o grupo amina (-NH2), com a superfície ativada do chip sensor (Nguyen et al., 2015).

Em casos que o ligante não apresenta grupos funcionais para se ligarem a superfície do *chip*, os mesmos podem ser alterados quimicamente e inseridos com por exemplo, grupo amina que no caso da utilização do CM5, se liga covalentemente com os grupos carboxílicos ativos e localizados na superfície do chip (Hudson et al., 2022). Ativar os grupos carboxílicos e posteriormente, bloquear aqueles que não interagiram com o grupo amina, faz parte do protocolo de análise e deve ser efetuado com atenção. Agentes bloqueadores inapropriados podem inativar as

biomoléculas. Além disso, a modificação química da biomolécula pode interferir na interação com o analito. Para situações de imobilização com moléculas ainda não relatadas pela literatura, testar diferentes químicas de imobilização é o caminho para a garantia da preservação da interação ligante-analito.

3.4 Experimento para obtenção da dinâmica de formação de complexo

Realizada a ativação dos grupos carboxílicos, imobilização da βLG na superfície do *chip* CM5, e bloqueio dos grupos ésteres reativos, os dados da dinâmica de formação de complexo βLG-RES podem ser obtidos pela adição de soluções com diferentes concentrações de RES. Estas, que interagem com a βLG e ocasionam a redução no valor do índice de refração na superfície do *chip* sensor (Sandoval-Altamirano et al., 2017).

Para expressar a mudança no índice de refração, após cada injeção da solução de RES sobre o *chip* sensor, é gerado um sinal de resposta ressonante (RU) em função do tempo, o chamado sensograma (Figura 4).

Figura 4 - Exemplo de sensograma (RU x Tempo) de uma interação proteína-analito, onde cada curva representa uma concentração do analito.

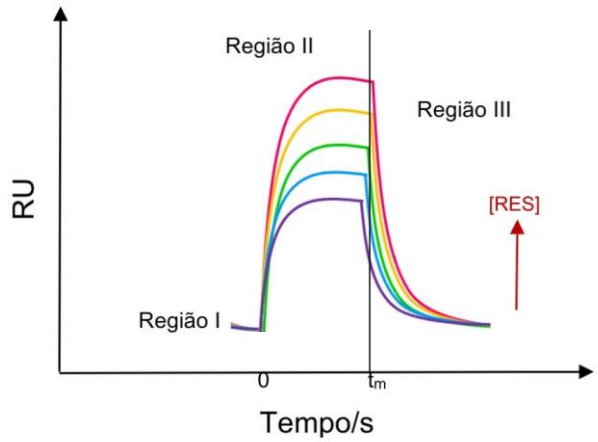

Fonte: Autora, 2022.

Como observado na Figura 4, o sensograma apresenta três regiões principais. Na região I, os sinais de SPR são aproximadamente zero e são provenientes apenas da presença de tampão fluindo sobre as células de referência e de amostra. Na

Região II, a partir de 0 s, dá-se o início das injeções com concentrações crescentes de RES. Assim, o sinal de SPR cresce até alcançar um valor experimental máximo e leva em consideração processos de associação de moléculas livres e dissociação do complexo termodinamicamente estável. Na Região III, os valores de RU decrescem em virtude apenas da presença de tampão fluindo na superfície do *chip* sensor e contribuindo para a dissociação espontânea do complexo e retorno à linha de base, a chamada fase de dissociação (Coelho et al., 2019; Nunes et al., 2019).

A interação entre uma proteína (βLG) e um analito (RES) pode ser considerada uma reação de interação monovalente, (βLG + RES ↔ βLG-RES), com constante de associação (k_a) e dissociação (k_d). Utilizando dados do sensograma, valores de k_{obs} e de k_d podem ser calculados de acordo com as Equações (1) e (2), (de Paula et al., 2017).

$$\mathrm{RU\ (t)} = \mathrm{RU_{máx}(t_\infty)}\left[1 - \mathrm{e^{-k_{obs}(t)}}\right] \quad (1)$$

$$\mathrm{RU\ (t)} = \mathrm{RU\ (t_m)\ e^{-k_d(t-t_m)}} \quad (2)$$

Em que t_m é o tempo em que a curva começa a decrescer, RU (t) é a resposta ressonante obtida em cada tempo t, $RU_{máx}$ (t_∞) é a resposta ressonante máxima, ou seja, quando a βLG é totalmente saturada pelo RES e, RU (t_m) é a resposta obtida no tempo t_m.

Em baixas concentrações de RES, o valor de k_{obs} é linearmente dependente da concentração deste. Assim, o valor de k_a pode ser obtido por meio da inclinação da curva do gráfico de k_{obs} versus [RES], Equação (3).

$$\mathrm{K_{obs}} = \mathrm{k_a\ [RES]} + \mathrm{k_d} \quad (3)$$

Para o cálculo da energia de ativação de associação ($E^{\ddagger}_{ativ\,(a)}$) ou dissociação ($E^{\ddagger}_{ativ\,(d)}$) do processo de formação de complexo ativado, o experimento de SPR deve ser realizado em diferentes temperaturas e posteriormente, o gráfico de Arrhenius construído por meio da plotagem de ln k_a ou ln k_d versus 1/T, Equação (4).

$$\mathrm{E_{ativ(y)}(T)} = -\mathrm{R}\left(\frac{\mathrm{d\ ln\ ln\ k(y)}}{\mathrm{dT}}\right) \quad (4)$$

Em que o subscrito ‘’y’’ poderá significar a fase de associação (a) ou de dissociação (d). $E^{\ddagger}_{ativ\,(y)}$ é a energia de ativação (kJ.mol^{-1}), R é a constante universal dos gases (8,3145 J.mol^{-1}.K^{-1}) e k_y é a constante de associação (k_a) ou dissociação (k_d) em M^{-1}.s^{-1} e s^{-1}, respectivamente.

Determinado o valor da $E^{\ddagger}_{ativ\,(y)}$, os valores da variação da energia livre de Gibbs de ativação ($\Delta G^{\ddagger}_{y}$), da variação da entalpia de ativação ($\Delta H^{\ddagger}_{y}$) e da variação da entropia de ativação $\left(T\Delta S^{\ddagger}_{y}\right)$ para a formação de complexo ativado a partir da associação de moléculas livres (y = a) ou da dissociação do complexo (y = d), podem ser calculados através das equações 5, 6 e 7, respectivamente.

$$k_y = \frac{k_B T}{h} exp - \left(\frac{\Delta G^{\ddagger}_{y}}{RT}\right) \tag{5}$$

$$\Delta \mathrm{H}^{\ddagger}_{\mathrm{y}}(\mathrm{T}) = \mathrm{E}_{\mathrm{ativ(y)}}(\mathrm{T}) - \mathrm{RT} \tag{6}$$

$$\mathrm{T}\Delta \mathrm{S}^{\ddagger}_{\mathrm{y}}(\mathrm{T}) = \Delta \mathrm{H}^{\ddagger}_{\mathrm{y}}(\mathrm{T}) - \Delta \mathrm{G}^{\ddagger}_{\mathrm{y}}(\mathrm{T}) \tag{7}$$

Onde h é a constante de Planck (6,62608 × 10^{-34} J.s).

Para o cálculo dos parâmetros termodinâmicos, considera-se a dependência da constante de ligação (K_b) com a temperatura. Assim, o valor de K_b pode ser obtido pela relação $K_b = k_a/k_d$. Os valores para a variação da energia livre de Gibbs ($\Delta G°$), entalpia ($\Delta H°$) e entropia ($T\Delta S°$) padrão de formação de complexo, podem ser calculados pelo intermédio das equações 8, 9 e 10.

$$\Delta G° = -RTlnK_b \tag{8}$$

$$\Delta H° = -R\frac{\partial(ln\,K_b)}{\partial(\frac{1}{T})} \tag{9}$$

$$T\Delta S° = \Delta H° - \Delta G° \tag{10}$$

Os parâmetros termodinâmicos de formação do complexo são úteis para entender sobre a estabilidade dos complexos e para avaliar as forças motrizes que

estão envolvidas na formação destes (Coelho et al., 2019; Hudson et al., 2022; Rezende et al., 2020).

4. Referências bibliográficas

ACD/ChemSketch, version 2019.2.0, Advanced Chemistry Development, Inc., Toronto, 387 ON, Canada, www.acdlabs.com, 2021

Amri, A., Chaumeil, J. C., Sfar, S., & Charrueau, C. (2012). Administration of resveratrol: What formulation solutions to bioavailability limitations? In *Journal of Controlled Release* (Vol. 158, Issue 2, pp. 182–193). https://doi.org/10.1016/j.jconrel.2011.09.083

Arcanjo, N. M. O., Luna, C., Madruga, M. S., & Estévez, M. (2018). Antioxidant and pro-oxidant actions of resveratrol on human serum albumin in the presence of toxic diabetes metabolites: Glyoxal and methyl-glyoxal. *Biochimica et Biophysica Acta (BBA) - General Subjects*, *1862*(9), 1938–1947. https://doi.org/10.1016/j.bbagen.2018.06.007

Bello, M., Gutiérrez, G., & García-Hernández, E. (2012). Structure and dynamics of β-lactoglobulin in complex with dodecyl sulfate and laurate: A molecular dynamics study. *Biophysical Chemistry*, *165-166*, 79–86. https://doi.org/10.1016/j.bpc.2012.03.009

Bourassa, P., Kanakis, C. D., Tarantilis, P., Pollissiou, M. G., & Tajmir-Riahi, H. A. (2010). Resveratrol, genistein, and curcumin bind bovine serum albumin. *Journal of Physical Chemistry B*, *114*(9), 3348–3354. https://doi.org/10.1021/JP9115996/asset/images/medium/jp-2009-115996_0008.gif

Brownlow, S., Morais Cabral, J. H., Cooper, R., Flower, D. R., Yewdall, S. J., Polikarpov, I., North, A. C., & Sawyer, L. (1997). Bovine beta-lactoglobulin at 1.8 A resolution--still an enigmatic lipocalin. *Structure (London, England : 1993)*, *5*(4), 481–495. https://doi.org/10.1016/S0969-2126(97)00205-0

Burns, J., Yokota, T., Ashihara, H., Lean, M. E. J., & Crozier, A. (2002). Plant foods and herbal sources of resveratrol. *Journal of Agricultural and Food Chemistry*, *50*(11), 3337–3340. https://doi.org/10.1021/jf0112973

Cao, S., Wang, D., Tan, X., & Chen, J. (2009). Interaction Between Trans-resveratrol and Serum Albumin in Aqueous Solution. *Journal of Solution Chemistry 2009*

38:9, *38*(9), 1193–1202. https://doi.org/10.1007/S10953-009-9439-7

Chain, C. Y., Daza Millone, M. A., Cisneros, J. S., Ramirez, E. A., & Vela, M. E. (2021). Surface Plasmon Resonance as a Characterization Tool for Lipid Nanoparticles Used in Drug Delivery. *Frontiers in Chemistry*, *8*(January), 1–9. https://doi.org/10.3389/fchem.2020.605307

Chen, J.-Y., Zhu, Q., Zhang, S., OuYang, D., & Lu, J.-H. (2019). Resveratrol in experimental Alzheimer's disease models: A systematic review of preclinical studies. *Pharmacological Research*, 104476. https://doi.org/10.1016/j.phrs.2019.104476

Cheng, H., Dong, H., Wusigale, & Liang, L. (2020). A comparison of β-casein complexes and micelles as vehicles for trans-/cis-resveratrol. *Food Chemistry*, *330*, 127209. https://doi.org/10.1016/j.foodchem.2020.127209

Cheng, H., Fang, Z., Wusigale, Bakry, A. M., Chen, Y., & Liang, L. (2018). Complexation of trans- and cis-resveratrol with bovine serum albumin, β-lactoglobulin or α-lactalbumin. *Food Hydrocolloids*, *81*, 242–252. https://doi.org/10.1016/j.foodhyd.2018.02.037

Coelho, Y. L., de Paula, H. M. C., Agudelo, A. J. P., de Castro, A. S. B., Hudson, E. A., Pires, A. C. S., & Silva, L. H. M. (2019). Lactoferrin-phenothiazine dye interactions: Thermodynamic and kinetic approach. *International Journal of Biological Macromolecules*, *136*, 559–569. https://doi.org/10.1016/j.ijbiomac.2019.06.097

Dai, T., Li, R., Liu, C., Liu, W., Li, T., Chen, J., Kharat, M., & McClements, D. J. (2019). Effect of rice glutelin-resveratrol interactions on the formation and stability of emulsions: A multiphotonic spectroscopy and molecular docking study. *Food Hydrocolloids*, *97*, 105234. https://doi.org/10.1016/j.foodhyd.2019.105234

De Paula, H. M. C., Coelho, Y. L., Agudelo, A. J. P., Rezende, J. de P., Ferreira, G. M. D., Ferreira, G. M. D., Pires, A. C. dos S., & da Silva, L. H. M. (2017). Kinetics and thermodynamics of bovine serum albumin interactions with Congo red dye. *Colloids and Surfaces B: Biointerfaces*, *159*, 737–742. https://doi.org/10.1016/j.colsurfb.2017.08.036

Dima, I. G., Aprodu, I., Râpeanu, G., & Stănciuc, N. (2018). Binding mechanisms between lycopene extracted from tomato peels and bovine β-lactoglobulin. *Journal of Luminescence*, *203*(April), 582–589.

https://doi.org/10.1016/j.jlumin.2018.07.017

Fan, Y., Liu, Y., Gao, L., Zhang, Y., & Yi, J. (2018). Improved chemical stability and cellular antioxidant activity of resveratrol in zein nanoparticle with bovine serum albumin-caffeic acid conjugate. *Food Chemistry*, *261*, 283–291. https://doi.org/10.1016/j.foodchem.2018.04.055

Gade, A., Sharma, A., Srivastava, N., & Flora, S. J. S. (2022). Surface plasmon resonance: A promising approach for label-free early cancer diagnosis. *Clinica Chimica Acta*, *527*(January), 79–88. https://doi.org/10.1016/j.cca.2022.01.023

Ghalandari, B., Divsalar, A., Saboury, A. A., Haertlé, T., Parivar, K., Bazl, R., Eslami-Moghadam, M., & Amanlou, M. (2014). Spectroscopic and theoretical investigation of oxali–palladium interactions with β-lactoglobulin. *Spectrochimica Acta Part A: Molecular and Biomolecular Spectroscopy*, *118*, 1038–1046. https://doi.org/10.1016/j.saa.2013.09.126

Guo, Y., & Jauregi, P. (2018). Protective effect of β-lactoglobulin against heat induced loss of antioxidant activity of resveratrol. *Food Chemistry*, *266*, 101–109. https://doi.org/10.1016/j.foodchem.2018.05.108

Habibian-Dehkordi, S., Farhadian, S., Ghasemi, M., & Evini, M. (2022). Insight into the binding behavior, structure, and thermal stability properties of β-lactoglobulin/Amoxicillin complex in a neutral environment. *Food Hydrocolloids*, *133*, 107830. https://doi.org/10.1016/j.foodhyd.2022.107830

Hailu, Y., Hansen, E. B., Seifu, E., Eshetu, M., Ipsen, R., & Kappeler, S. (2016). Functional and technological properties of camel milk proteins: A review. *Journal of Dairy Research*, *83*(4), 422–429. https://doi.org/10.1017/S0022029916000686

Huang, X., Li, X., Xie, M., Huang, Z., Huang, Y., Wu, G., Peng, Z., Sun, Y., Ming, Q., Liu, Y., Chen, J., & Xu, S. (2019). Resveratrol: Review on its discovery, anti-leukemia effects and pharmacokinetics. *Chemico-Biological Interactions*, *306*, 29–38. https://doi.org/10.1016/j.cbi.2019.04.001

Hudson, E., Campos de Paula, H. M., Coelho, Y. L., Glanzmann, N., da Silva, A. D., Mendes da Silva, L. H., & dos Santos Pires, A. C. (2022). The kinetics of formation of resveratrol-β-cyclodextrin-NH2 and resveratrol analog-β-cyclodextrin-NH2 supramolecular complexes. *Food Chemistry*, *366*, 130612. https://doi.org/10.1016/j.foodchem.2021.130612

Jebelli, A., Oroojalian, F., Fathi, F., Mokhtarzadeh, A., & Guardia, M. de la. (2020). Recent advances in surface plasmon resonance biosensors for microRNAs

detection. *Biosensors and Bioelectronics*, *169*(July), 112599. https://doi.org/10.1016/j.bios.2020.112599

Jiang, Y. L. (2008). Design, synthesis and spectroscopic studies of resveratrol aliphatic acid ligands of human serum albumin. *Bioorganic & Medicinal Chemistry*, *16*(12), 6406–6414. https://doi.org/10.1016/J.BMC.2008.05.002

Katsamba, P. S., Park, S., & Laird-Offringa, I. A. (2002). Kinetic studies of RNA-protein interactions using surface plasmon resonance. *Methods*, *26*(2), 95–104. https://doi.org/10.1016/S1046-2023(02)00012-9

Kurpiewska, K., Biela, A., Loch, J. I., Lipowska, J., Siuda, M., & Lewiński, K. (2019). Towards understanding the effect of high pressure on food protein allergenicity: β-lactoglobulin structural studies. *Food Chemistry*, *270*, 315–321. https://doi.org/10.1016/j.foodchem.2018.07.104

Lajnaf, R., Picart-Palmade, L., Attia, H., Marchesseau, S., & Ayadi, M. A. (2022). Foaming and air-water interfacial properties of camel milk proteins compared to bovine milk proteins. *Food Hydrocolloids*, *126*, 107470. https://doi.org/10.1016/j.foodhyd.2021.107470

Lelis, C. A., Nunes, N. M., de Paula, H. M. C., Coelho, Y. L., da Silva, L. H. M., & Pires, A. C. dos S. (2020). Insights into protein-curcumin interactions: Kinetics and thermodynamics of curcumin and lactoferrin binding. *Food Hydrocolloids*, *105*, 105825. https://doi.org/10.1016/j.foodhyd.2020.105825

Liang, L., & Subirade, M. (2012). Study of the acid and thermal stability of β-lactoglobulin–ligand complexes using fluorescence quenching. *Food Chemistry*, *132*(4), 2023–2029. https://doi.org/10.1016/J.FOODCHEM.2011.12.043

Liang, L., Tajmir-Riahi, H. A., & Subirade, M. (2008). Interaction of β-Lactoglobulin with resveratrol and its biological implications. *Biomacromolecules*, *9*(1), 50–56. https://doi.org/10.1021/BM700728K

Liang, Q., Ren, X., Zhang, X., Hou, T., Chalamaiah, M., Ma, H., & Xu, B. (2018). Effect of ultrasound on the preparation of resveratrol-loaded zein particles. *Journal of Food Engineering*, *221*, 88–94. https://doi.org/10.1016/j.jfoodeng.2017.10.002

Lin, J. A., Kuo, C. H., Chen, B. Y., Li, Y., Liu, Y. C., Chen, J. H., & Shieh, C. J. (2016). A novel enzyme-assisted ultrasonic approach for highly efficient extraction of resveratrol from Polygonum cuspidatum. *Ultrasonics Sonochemistry*, *32*, 258–264. https://doi.org/10.1016/j.ultsonch.2016.03.018

Liu, Q., Qin, Y., Jiang, B., Chen, J., & Zhang, T. (2022). Development of self-assembled zein-fucoidan complex nanoparticles as a delivery system for resveratrol. *Colloids and Surfaces B: Biointerfaces*, *216*, 112529. https://doi.org/10.1016/J.colsurfb.2022.112529

Loch, J. I., Bonarek, P., Polit, A., Jabłoński, M., Czub, M., Ye, X., & Lewiński, K. (2015). β-Lactoglobulin interactions with local anaesthetic drugs – Crystallographic and calorimetric studies. *International Journal of Biological Macromolecules*, *80*, 87–94. https://doi.org/10.1016/J.IJBIOMAC.2015.06.013

López-Nicolás, J. M., & García-Carmona, F. (2008). Aggregation state and pKa values of (E)-resveratrol as determined by fluorescence spectroscopy and UV-visible absorption. *Journal of Agricultural and Food Chemistry*, *56*(17), 7600–7605. https://doi.org/10.1021/jf800843e

Lu, Z., Zhang, Y., Liu, H., Yuan, J., Zheng, Z., & Zou, G. (2007). Transport of a Cancer Chemopreventive Polyphenol, Resveratrol: Interaction with Serum Albumin and Hemoglobin. *Journal of Fluorescence 2007 17:5*, *17*(5), 580–587. https://doi.org/10.1007/S10895-007-0220-2

Mansouri, M., Fathi, F., Jalili, R., Shoeibie, S., Dastmalchi, S., Khataee, A., & Rashidi, M. R. (2020). SPR enhanced DNA biosensor for sensitive detection of donkey meat adulteration. *Food Chemistry*, *331*, 127163. https://doi.org/10.1016/j.foodchem.2020.127163

Miyazaki, C. M., & Shimizu, F. M. (2017). Surface Plasmon Resonance (SPR) for Sensors and Biosensors. *Nanocharacterization Techniques*, 183–200. https://doi.org/10.1016/B978-0-323-49778-7.00006-0

N′ soukpoé-Kossi, C. N., St-Louis, C., Beauregard, M., Subirade, M., Carpentier, R., Hotchandani, S., & Tajmir-Riahi, H. A. (2006). Resveratrol binding to human serum albumin. *Journal of Biomolecular Structure & Dynamics*, *24*(3), 277–283. https://doi.org/10.1080/07391102.2006.10507120

Nair, M. S. (2015). Spectroscopic study on the interaction of resveratrol and pterostilbene with human serum albumin. *Journal of Photochemistry and Photobiology B: Biology*, *149*, 58–67. https://doi.org/10.1016/j.jphotobiol.2015.05.001

Nguyen, H. H., Park, J., Kang, S., & Kim, M. (2015). Surface plasmon resonance: A versatile technique for biosensor applications. In *Sensors (Switzerland)* (Vol. 15, Issue 5, pp. 10481–10510). MDPI AG. https://doi.org/10.3390/s150510481

Nunes, N. M., de Paula, H. M. C., Coelho, Y. L., da Silva, L. H. M., & Pires, A. C. S. (2019). Surface plasmon resonance study of interaction between lactoferrin and naringin. *Food Chemistry*, *297*, 125022. https://doi.org/10.1016/j.foodchem.2019.125022

Ojaghian, M. R., Wang, Q., Li, X., Sun, X., Xie, G. L., Zhang, J., Hai-Wei, F., & Wang, L. (2016). Inhibitory effect and enzymatic analysis of E-cinnamaldehyde against sclerotinia carrot rot. *Pesticide Biochemistry and Physiology*, *127*, 8–14. https://doi.org/10.1016/j.pestbp.2015.08.005

Olsen, K., Orlien, V., & Skibsted, L. H. (2022). Pressure denaturation of β-lactoglobulin: Volume changes for genetic A and B variants. *International Dairy Journal*, *133*, 105416. https://doi.org/10.1016/j.idairyj.2022.105416

Pantusa, M., Sportelli, L., & Bartucci, R. (2012). Influence of stearic acids on resveratrol-HSA interaction. *European Biophysics Journal 2012 41:11*, *41*(11), 969–977. https://doi.org/10.1007/S00249-012-0856-Y

Poór, M., Kaci, H., Bodnárová, S., Mohos, V., Fliszár-Nyúl, E., Kunsági-Máté, S., Özvegy-Laczka, C., & Lemli, B. (2022). Interactions of resveratrol and its metabolites (resveratrol-3-sulfate, resveratrol-3-glucuronide, and dihydroresveratrol) with serum albumin, cytochrome P450 enzymes, and OATP transporters. *Biomedicine & Pharmacotherapy*, *151*, 113136. https://doi.org/10.1016/j.biopha.2022.113136

Pujara, N., Jambhrunkar, S., Wong, K. Y., McGuckin, M., & Popat, A. (2017). Enhanced colloidal stability, solubility and rapid dissolution of resveratrol by nanocomplexation with soy protein isolate. *Journal of Colloid and Interface Science*, *488*, 303–308. https://doi.org/10.1016/j.jcis.2016.11.015

Ramalingam, S., Collier, C. M., & Singh, A. (2021). A Paper-Based Colorimetric Aptasensor for the Detection of Gentamicin. *Biosensors*, *11*(2). https://doi.org/10.3390/BIOS11020029

Ravindran, N., Kumar, S., Yashini, M., Rajeshwari, S., Mamathi, C. A., Nirmal Thirunavookarasu, S., & Sunil, C. K. (2021). Recent advances in Surface Plasmon Resonance (SPR) biosensors for food analysis: a review. *Critical Reviews in Food Science and Nutrition*, *0*(0), 1–23. https://doi.org/10.1080/10408398.2021.1958745

Rezende, J. de P., Hudson, E. A., De Paula, H. M. C., Meinel, R. S., Da Silva, A. D., Da Silva, L. H. M., & Pires, A. C. dos S. (2020). Human serum albumin-

resveratrol complex formation: Effect of the phenolic chemical structure on the kinetic and thermodynamic parameters of the interactions. *Food Chemistry*, *307*, 125514. https://doi.org/10.1016/j.foodchem.2019.125514

Robinson, K., Mock, C., & Liang, D. (2015). Pre-formulation studies of resveratrol. *Drug Development and Industrial Pharmacy*, *41*(9), 1464–1469. https://doi.org/10.3109/03639045.2014.958753

Sandoval-Altamirano, C., Sanchez, S. A., Ferreyra, N. F., & Gunther, G. (2017). Understanding the interaction of concanavalin a with mannosyl glycoliposomes: A surface plasmon resonance and fluorescence study. *Colloids and Surfaces B: Biointerfaces*, *158*, 539–546. https://doi.org/10.1016/j.colsurfb.2017.07.026

Santos, A. C., Pereira, I., Pereira-Silva, M., Ferreira, L., Caldas, M., Magalhães, M., Figueiras, A., Ribeiro, A. J., & Veiga, F. (2019). Nanocarriers for resveratrol delivery: Impact on stability and solubility concerns. *Trends in Food Science & Technology*, *91*, 483–497. https://doi.org/10.1016/j.tifs.2019.07.048

Schneider, C. S., Bhargav, A. G., Perez, J. G., Wadajkar, A. S., Winkles, J. A., Woodworth, G. F., & Kim, A. J. (2015). Surface plasmon resonance as a high throughput method to evaluate specific and non-specific binding of nanotherapeutics. *Journal of Controlled Release*, *219*, 331–344. https://doi.org/10.1016/j.jconrel.2015.09.048

Situ, C., Mooney, M. H., Elliott, C. T., & Buijs, J. (2010). Advances in surface plasmon resonance biosensor technology towards high-throughput, food-safety analysis. *TrAC - Trends in Analytical Chemistry*, *29*(11), 1305–1315. https://doi.org/10.1016/j.trac.2010.09.003

Sorel Muresan, Arie van der Bent, and, & Wolf*, F. A. de. (2001). *Interaction of β-Lactoglobulin with Small Hydrophobic Ligands As Monitored by Fluorometry and Equilibrium Dialysis: Nonlinear Quenching Effects Related to Protein−Protein Association*. https://doi.org/10.1021/jf0012188

Świątek, S., Komorek, P., Turner, G., & Jachimska, B. (2019). β-Lactoglobulin as a potential carrier for bioactive molecules. *Bioelectrochemistry*, *126*, 137–145. https://doi.org/10.1016/j.bioelechem.2018.12.006

Taulier, N., & Chalikian, T. V. (2001). Characterization of pH-induced transitions of β-lactoglobulin: ultrasonic, densimetric, and spectroscopic studies. *Journal of Molecular Biology*, *314*(4), 873–889. https://doi.org/10.1006/JMBI.2001.5188

Vachali, P. P., Li, B., Bartschi, A., & Bernstein, P. S. (2015). Surface plasmon

resonance (SPR)-based biosensor technology for the quantitative characterization of protein-carotenoid interactions. In *Archives of Biochemistry and Biophysics* (Vol. 572, pp. 66–72). Academic Press Inc. https://doi.org/10.1016/j.abb.2014.12.005

Vale, R. T. R., de Paula, H. M. C., Coelho, Y. L., Rezende, J. D. P., Vidigal, M. C. T. R., Da Silva, L. H. M., & Pires, A. C. D. S. (2022). β-lactoglobulin and resveratrol nanocomplex formation is driven by solvation water release. *Food Research International*, *158*, 111567. https://doi.org/10.1016/j.foodres.2022.111567

Vijayalakshmi, L., Krishna, R., Sankaranarayanan, R., & Vijayan, M. (2008). An asymmetric dimer of beta-lactoglobulin in a low humidity crystal form--structural changes that accompany partial dehydration and protein action. *Proteins*, *71*(1), 241–249. https://doi.org/10.1002/prot.21695

Vikas, Yadav, M. K., Kumar, P., & Verma, R. K. (2020). Detection of adulteration in pure honey utilizing Ag-graphene oxide coated fiber optic SPR probes. *Food Chemistry*, *332*, 127346. https://doi.org/10.1016/J.FOODCHEM.2020.127346

Wang, C., Chen, L., Lu, Y., Liu, J., Zhao, R., Sun, Y., Sun, B., & Cuina, W. (2021). pH-Dependent complexation between β-lactoglobulin and lycopene: Multi-spectroscopy, molecular docking and dynamic simulation study. *Food Chemistry*, *362*(May), 130230. https://doi.org/10.1016/j.foodchem.2021.130230

Wusigale, Fang, Z., Hu, L., Gao, Y., Li, J., & Liang, L. (2017). Protection of resveratrol against the photodecomposition of folic acid and photodecomposition-induced structural change of beta-lactoglobulin. *Food Research International*, *102*, 435–444. https://doi.org/10.1016/j.foodres.2017.09.006

Xu, Y., Wu, J., & Wang, S. (2021). Comparative study of whey protein isolate and gelatin treated by pH-shifting combined with ultrasonication in loading resveratrol. *Food Hydrocolloids*, *117*, 106694. https://doi.org/10.1016/j.foodhyd.2021.106694

Yesudasu, V., Pradhan, H. S., & Pandya, R. J. (2021). Recent progress in surface plasmon resonance based sensors: A comprehensive review. *Heliyon*, *7*(3), e06321. https://doi.org/10.1016/j.heliyon.2021.E06321

Yi, J., He, Q., Peng, G., & Fan, Y. (2022). Improved water solubility, chemical stability, antioxidant and anticancer activity of resveratrol via nanoencapsulation with pea protein nanofibrils. *Food Chemistry*, *377*, 131942.

https://doi.org/10.1016/j.foodchem.2021.131942

Zagury, Y., Kazir, M., & Livney, Y. D. (2019). Improved antioxidant activity, bioaccessibility and bioavailability of EGCG by delivery in β-lactoglobulin particles. *Journal of Functional Foods*, *52*, 121–130. https://doi.org/10.1016/J.JFF.2018.10.025

Zhang, P., Chen, Y. P., & Guo, J. S. (2021). SPR for water pollutant detection and water process analysis. *Comprehensive Analytical Chemistry*, *95*, 145–183. https://doi.org/10.1016/bs.coac.2021.06.001

Zhang, X., Lu, Y., Zhao, R., Wang, C., Wang, C., & Zhang, T. (2022). Study on simultaneous binding of resveratrol and curcumin to β-lactoglobulin: Multi-spectroscopic, molecular docking and molecular dynamics simulation approaches. *Food Hydrocolloids*, *124*, 107331. https://doi.org/10.1016/j.foodhyd.2021.107331

Zhou, J., Qi, Q., Wang, C., Qian, Y., Liu, G., Wang, Y., & Fu, L. (2019). Surface plasmon resonance (SPR) biosensors for food allergen detection in food matrices. *Biosensors and Bioelectronics*, *142*(April), 111449. https://doi.org/10.1016/j.bios.2019.111449

Zhu, J., Li, K., Wu, H., Li, W., & Sun, Q. (2020). Multi-spectroscopic, conformational, and computational atomic-level insights into the interaction of β-lactoglobulin with apigenin at different pH levels. *Food Hydrocolloids*, *105*, 105810. https://doi.org/10.1016/j.foodhyd.2020.105810

CAPÍTULO 2: β-lactoglobulin and resveratrol nanocomplex formation is driven by solvation water release

Article Published in: Food Research International
https://doi.org/10.1016/j.foodres.2022.111567

Received date: 19 April 2022
Revised date: 14 June 2022
Accepted date: 22 June 2022

β-lactoglobulin and resveratrol nanocomplex formation is driven by solvation water release

Rafaela Teixeira Rodrigues do Vale[a], Hauster Maximiler Campos de Paula[b], Yara Luiza Coelho[b], Jaqueline De Paula Rezende[c], Márcia Cristina Teixeira Ribeiro Vidigal[a], Luis Henrique Mendes Da Silva[b*], Ana Clarissa Dos Santos Pires[a**]

[a] Applied Molecular Thermodynamics Group (THERMA), Department of Food Technology, Federal University of Viçosa, Av. P. H. Rolfs s/n, Viçosa, MG, Brazil, 36570900

[b] Colloidal and Macromolecular Green Chemistry Group (QUIVECOM), Department of Chemistry, Federal University of Viçosa, Av. P. H. Rolfs s/n, Viçosa, MG, Brazil, 36570900

[c] Food Science Department, Federal University of Lavras, Av. Doutor Sylvio Menicucci, s/n, Campus UFLA, Lavras, MG, Brazil, 37200-900

Corresponding author: * luhen@ufv.br, phone: + 55 31 36126633, Fax: +55 31 36126600; ** ana.pires@ufv.br, phone: + 55 31 36126720, Fax: + 55 31 36126702

Highlights

- Thermodynamically stable complexes are formed through activated complexes.
- The water molecules of the desolvation layer influence the association.
- The interaction causes a conformational change at the beta-lactoglobulin site.
- At the low temperature (285.15 K) the hydrophobic interaction prevails.
- At high temperatures (301.15 K), hydrophilic interactions are dominant.

Graphical abstract

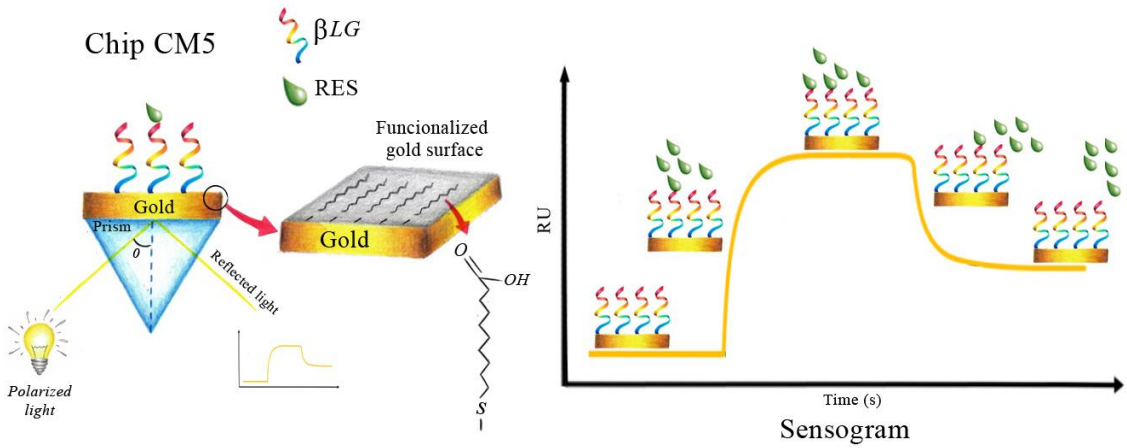

Abstract

Despite some thermodynamics studies about β-lactoglobulin (βLG) and resveratrol (RES) interactions, there is a gap regarding kinetics data about RES-βLG complex formation. Here, we determined the kinetic and thermodynamic parameters of RES-βLG interactions by using surface plasmon resonance (SPR). The kinetic association parameters were dependent on the 3D water structure present on the solvation shell of both interacting molecules. At lower temperature (285.15 K), all activation energies were positive ($E^{\ddagger}_{act\,(a)} = 82.86$ kJ.mol^{-1}, $T\Delta S^{\ddagger}_{a} = 32.26$ kJ.mol^{-1}, and $\Delta C^{\ddagger}_{p\,(a)} = 4.15$ kJ.mol^{-1}k^{-1}) due to the higher water structuration on the RES and βLG solvation shell. All these energetic barriers become mainly from the energetic cost for the desolvation process of RES and βLG. At higher temperature (301.15 K), the solvation water structure decreases and all the above activation energies become negative ($E^{\ddagger}_{act\,(a)} = -121.58$ kJ.mol^{-1}, $T\Delta S^{\ddagger}_{a} = -173.59$ kJ.mol^{-1}, and $\Delta C^{\ddagger}_{p\,(a)} = -29.92$ kJ.mol^{-1}k^{-1}) because the direct interaction between desolvated RES and βLG molecules released more energy than it is absorbed by desolvation process. However, kinetic dissociation parameters were not dependent on the hydrogen bond density of the water solvation shell as showed by the temperature independence of dissociation energetic parameters. This non-dependence of the dissociation process from the desolvation step probably is because the water molecules interacting with the RES-βLG complex is not concentrated around/inside the protein site of interaction. The association of free molecules was 1.5 times faster than the dissociation of the thermodynamically stable complex ($\Delta G^{\ddagger}_{(a)} \cong 48.15$ kJ.mol^{-1}, $\Delta G^{\ddagger}_{(d)} \cong 73.10$ kJ.mol^{-1}). The lower free energy barrier observed for the association came from an isokinetic process where entropic and enthalpic parameters compensated for each other. The ΔG° values indicate that the thermodynamically stable complex predominates over free molecules. At low temperature (285.15 K), the hydrophobic interaction (ΔH° = 73.06 kJ.mol^{-1}; TΔS° = 99.60 kJ.mol^{-1}) drove the RES-βLG complex formation while at high temperature (301.15 K), hydrophilic interactions became dominant (ΔH° = -142.50 kJ.mol^{-1}; TΔS° = -118.18 kJ.mol^{-1}).

Keywords: Protein, polyphenol, intermolecular interaction, nanocarrier

1. Introduction

Resveratrol (RES), a natural stilbene (Figure 1) found in grapes, blueberries, raspberries, blackberries, red wine, and chocolate, is among the most important and studied phenolic compounds (Kotta et al., 2021; Robertson et al., 2022). It exhibits anti-inflammatory, neuroprotective, cardioprotective, anti-carcinogenic, anti-aging, anti-diabetic, anti-obesity, and antioxidant activities (Chen et al., 2019). However, RES has poor water solubility (0.023 $mg.ml^{-1}$ at 298.15 K) and chemical stability against UV light and pH (Fan et al., 2018; Yi et al., 2022).

Figure 1 - Chemical structure of trans-resveratrol (3,5,4′-trihydroxystylbene).

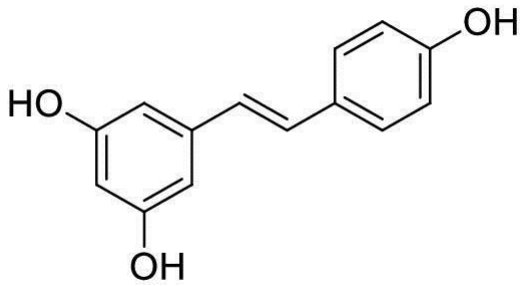

Resveratrol can form complexes with different proteins, such as pea proteins (Yi et al., 2022), zein (Liang et al., 2018; Liu et al., 2022), rice glutelin (Dai et al., 2019), soy protein isolate (Pujara et al., 2017), whey protein isolate (Xu et al., 2021), β-casein (Cheng et al., 2020), human serum albumin (Cao et al., 2009; Jiang, 2008; N′ soukpoé-Kossi et al., 2006; Nair, 2015; Pantusa et al., 2012; Poór et al., 2022; Rezende et al., 2020), bovine serum albumin (Arcanjo et al., 2018; Bourassa et al., 2010; Lu et al., 2007), α-lactalbumin (Cheng et al., 2018), and β-lactoglobulin (βLG) (Cheng et al., 2018; Guo & Jauregi, 2018; Liang & Subirade, 2012; Liang et al., 2008; Wusigale et al., 2017; Zhang et al., 2022), which affects the solubility and chemical, photo, and thermal stabilities of the phenolic compound. Among the proteins, βLG is one of the most essential transport proteins and is relevant to the pharmaceutical and food industries for the encapsulating, protecting, and delivering drugs and bioactive compounds (Dima et al., 2018; Wolf & Brett, 2000; Zhang et al., 2014). Guo and Jauregi (2018) investigated the thermal stability and antioxidant activity of RES complexed with βLG (native protein and nanoparticles) under heating conditions (348.15 K for 45 min). The free RES reduced the antioxidant capacity, which was

determined using the total antioxidant activity. Conversely, the antioxidant capacity (inhibition %) was improved (approximately 20 and 22.5% for βLG native form and nanoparticles, respectively) when RES (7 mg/100 mL) was complexed with βLG in native and nanoparticle forms.

Cheng et al. (2018) used circular dichroism, fluorescence spectroscopy (FS), and molecular simulation techniques to evaluate complex formation between βLG and *cis*- and *trans*-RES at pH 7.4. They observed a binding constant (K_b) on the order of 10^4 M^{-1}, with a stoichiometry (n) of 1.02, indicating that each binding site available for RES on βLG interacted with one *cis*- and *trans*-RES molecule. However, other thermodynamic parameters (such as, standard enthalpy, entropy, and Gibbs free energy change) that are crucial for understanding the complex formation mechanisms under different conditions have not been determined. Recently, Zhang et al. (2022) studied the isolated and simultaneous binding of the antioxidants resveratrol (RES) and curcumin (CUR) with bovine β-lactoglobulin (βLG), using multi-spectroscopic, molecular docking and molecular dynamics simulation approaches. Fluorescence spectra, FT-IR, CD, XRD and DSC spectra indicated that RES and CUR bind individually and simultaneously to βLG. Binding of RES with βLG improved the antioxidant activity of RES. The binding constant and stoichiometry values for the interaction between βLG and RES were 1.86×10^6 M^{-1} and 1.33 ± 0.02, respectively. However, the authors also did not present further thermodynamic data.

In addition to the lack of a complete thermodynamic analysis, data on the kinetics of complex formation between RES and βLG is unavailable. Nevertheless, determining the kinetic parameters of the βLG-RES complex formation may provide valuable information on the association rate of interacting molecules to form a complex and the dissociation rate of the complex. Furthermore, they provide insights into the molecular dynamics of complex formation (Hudson et al., 2022; Rezende et al., 2022).

Surface plasmon resonance (SPR) is a useful technique for monitoring and analyzing the dynamics of complex formation and occurrence of biomolecular interactions in real time, providing kinetic and thermodynamic data on complex formation. Additionally, SPR is label free in contrast to FS (Su et al., 2021). Therefore, we carried out a complete analysis (kinetic and thermodynamic) of RES-βLG complex formation at different temperatures and pH 7.4, using SPR.

2. Materials and methods

2.1 Materials

Solid standards of *trans*-RES (R5010) (≥ 99 %wt.) and βLG (≥ 90 %wt.) were purchased from Sigma-Aldrich (USA). Dibasic sodium phosphate (Na_2HPO_4) and sodium phosphate monohydrate ($NaH_2PO_4.H_2O$) were purchased from Vetec (Brazil). CM5 sensor chips and coupling reagents (N-ethyl-N'-(dimethylaminopropyl) carbodiimide (EDC), N-hydroxysuccinimide (NHS), and ethanolamine hydrochloride were purchased from GE Healthcare (USA). All the chemicals and reagents used in this study were of analytical grade.

2.2 Methods

2.2.1 Surface plasmon resonance (SPR) analysis

The kinetics and thermodynamics of βLG-RES interaction were assessed by SPR analysis using a Biacore X100 instrument (GE Healthcare, Pittsburgh, PA, USA) equipped with an automatic flow injection system. Three CM5 sensor chips were used in this study. Two flow channels were present on the CM5 surface: a sample channel (wherein βLG was immobilized) and a reference channel (without macromolecule immobilization). The SPR experiments were conducted in triplicate to ensure accuracy, and the results are expressed as the mean ± standard deviation.

2.2.2. Surface activation of CM5 sensor chip and immobilization of the βLG

Initially, carboxylic groups on the CM5's surface were activated by passing an EDC/NHS (0.4 M/0.1 M) mixture at a flow rate of 10 $\mu l.min^{-1}$ for 7 min. After activating the surface of the chip, the protein was immobilized using amine-coupling chemistry (Coelho et al., 2019). For protein immobilization, a βLG solution (30 $\mu g.mL^{-1}$, sodium acetate buffer (10 mM), pH 4) was injected into the sample cell at a flow rate of 10 $\mu L\ min^{-1}$ for 7 min and at 298.15 K. This procedure resulted in the low-density immobilization of βLG (3047 RU), which reduced mass transport and crowding phenomena. After the immobilization, the remaining reactive esters were blocked with ethanolamine for 7 min. Additionally, a reference flow cell was activated and

blocked, as described above, without protein immobilization to reduce systematic noise and Biacore drift.

2.2.3 RES-βLG interaction experiment by SPR

The RES-βLG interaction was analyzed at pH 7.4 and temperatures ranging from 285.15 to 301.15 K. Initially, the HBS-EP buffer (0.01 M HEPES pH 7.4, 0.15 M NaCl, and 0.005% v/v surfactant P20) and DMSO (4%, v/v) were injected into both the sample and reference channels of the CM5 sensor to obtain the baseline. Subsequently, RES solutions (20–70 μM, prepared in HBS-EP buffer + DMSO (4%, v/v) were injected into the flow system for 20 s at a flow rate of 10 μL min^{-1}. A sensorgram (RU *versus* time) was generated for each concentration of RES to characterize the binding cycle. After each binding cycle, the pure running buffer was injected again into both CM5 channels to dissociate the formed RES-βLG complexes and return them to baseline.

2.3 Statistical analysis

Mathematical models were obtained from the experimental data on kinetics and interaction thermodynamics to analyze the influence of temperature on each parameter, which were built using regression models. The observed differences were evaluated by analysis of variance (ANOVA), the significance of which was judged using the F test and a confidence level of p-value < 0.05. Statistical data were processed using OringinPro software version 8.0.

3. Results and discussion

3.1 SPR measurements

Surface plasmon resonance is a useful tool for analyzing the binding kinetics between proteins and polyphenols, such as RES, because models providing kinetic association and dissociation constants (related to protein-ligand binding processes) can be fitted to the data extracted from the resonant response (RU) *versus* time plot (sensorgram, Figure 2).

Figure 2 - Sensorgrams (RU *versus* time) for the binding of βLG-RES at 298.15 K with a protein immobilization density of 3047 RU. The direction of the arrow indicates an increase in the RES concentration (20, 30, 40, 50, 60, and 70 μM).

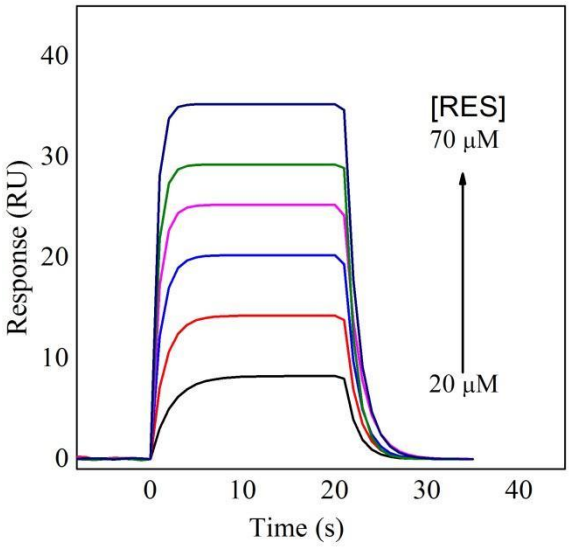

In Figure 2, each sensorgram indicates a specific concentration of RES solution that flowed over βLG (immobilized at 3047 RU). The obtained result is the difference between the RU of the sample (with immobilized protein) and reference (without protein immobilization) channels (Nguyen et al., 2015).

The sensorgram behavior can be interpreted as follows: initially, the RU signals were approximately zero until 0 s, resulting only from the presence of the buffer flowing over both the reference and sample channels and thereby causing almost an identical change in the refractive index. The RES solutions were injected by 0 s, resulting in an abrupt increase followed by constant values of the RU up to 20 s. This increase was attributed to the association between free RES and βLG molecules and the dissociation of a thermodynamically stable complex. However, it is important to note that the association rate at this stage was remarkably higher than the dissociation rate. The number of association and dissociation events were almost similar at the plateau (RU was almost constant over time). Finally, the RU signal decreased after 20 s and returned to the baseline because only the buffer flowed over the two channels; the dissociation of the thermodynamically stable complex was the dominant process. For all concentrations of RES and at all tested temperatures, the sensorgram profiles were similar (Figure 1S).

Figure 1S - Sensorgrams (RU vs. Time) for BLG-RES, 20-70 μM RES solutions flowing over a CM5 low-density HBLG-immobilized sensor-chip surface (3047 RU). (a) 285.15 K, (b) 289.15 K, (c) 293.15 K, (d) 297.15 K and, (e) 301.15 K.

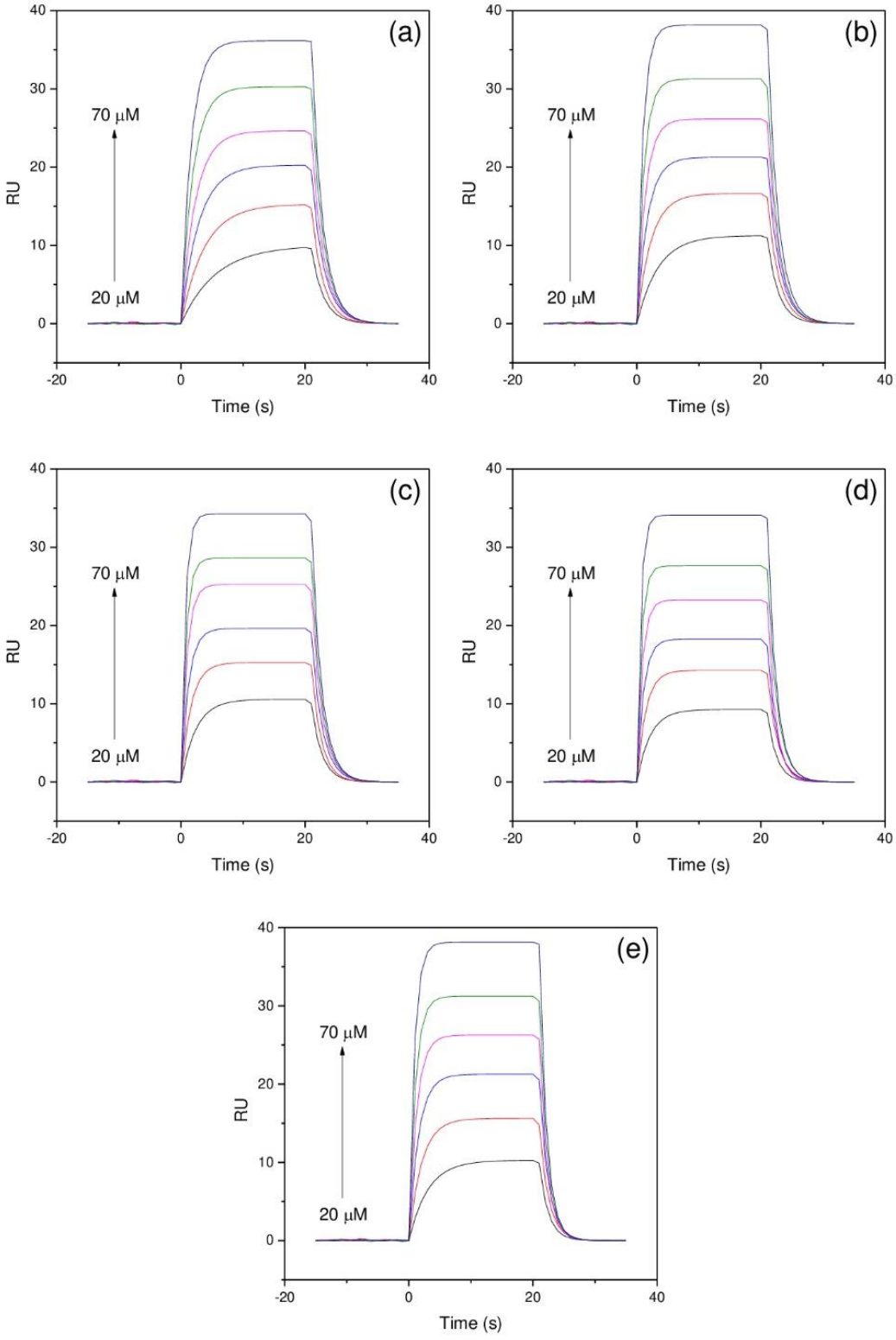

3.2 Kinetics of RES interaction with immobilized βLG

Understanding the kinetics of the βLG-RES complex formation process allowed us to determine the number of complexes formed and percentage of complexes dissociated at each second. This information can be obtained through the association (k_a) and dissociation (k_d) rate constants, and it is fundamental to apply this functional complex in different matrices.

The pseudo-first-order (Eq. (1)) and first-order (Eq. (2)) models were fitted globally to the data of the sensograms considering that the stoichiometry of complex formation between βLG-RES was 1:1 (Cheng et al., 2018). We then obtained the values of the observed kinetic constants (k_{obs}) and k_d.

$$RU\ (t) = RU_{máx}(t_\infty)\left[1 - e^{-k_{obs}(t)}\right] \quad (1)$$

$$RU\ (t) = RU\ (t_m)\ e^{-k_d(t-t_m)} \quad (2)$$

where t_m is the time at which the descendant curve begins, $RU\ (t)$ is the resonant response obtained at each time t, $RU_{máx}(t_\infty)$ is the maximum resonant response, that is, when βLG is fully saturated by the RES, and $RU\ (t_m)$ is the response obtained at time t_m.

The k_{obs} values were linearly dependent on the polyphenol concentration, considering the different tested temperatures tested and the low RES concentrations (Figure 2S). Therefore, the k_a values were determined from the slope of the plot k_{obs} *versus* [RES] plot (Eq. (3), Table 1).

$$k_{obs} = k_a\ [RES] + k_d \quad (3)$$

Figure 2S - Plot of K_{obs} as a function of RES concentration, used to determine k_a at temperatures: (■) 285.15 K, (●) 289.15 K, (▲) 293.15 K, (○) 297.15 K, (Δ) 298.15 K and (X) 301. 15 K.

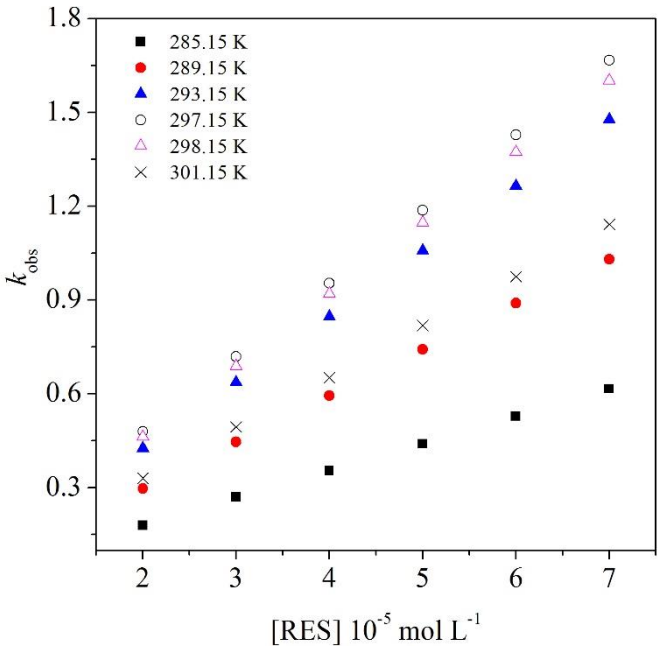

Table 1

Rate constants for the association (k_a) and dissociation (k_d) of βLG-RES interaction.

T	k_a*	k_d*
K	10^4 $M^{-1}s^{-1}$	s^{-1}
285.15	0.87	0.53
289.15	1.47	0.56
293.15	2.10	0.61
297.15	2.37	0.67
298.15	2.28	0.69
301.15	1.62	0.74

*Standard deviations of k_a and k_b at each temperature did not exceed 5%.

As shown in Table 1, an average of 17,900 complexes of the βLG-RES complex were formed at each second. Although a large amount of this functional supramolecular structure was formed, approximately 60% of the molecules dissociated at the same time interval.

Rezende et al. (2020) evaluated the complex formation between RES and human serum albumin (HSA) using the SPR technique under temperature and pH conditions similar to those in our present study; however, their obtained values of k_a and k_d were 19.1 and 2.7-fold lower than those in our present study, respectively. These results indicate that the RES and βLG interaction generates more number of complexes at each second than the RES and HSA interaction. The discrepancy between HSA and βLG could be related to the difference in the protein-binding sites of the RES. The three-dimensional (3D) structure of βLG, in a chalice form, is strongly influenced by changes in pH, for example, the inside of the βLG binding site becomes more accessible above pH 7.3. Thus, the association and dissociation of ligands are facilitated, consequently influencing the high values of k_a and k_d (Vijayalakshmi et al., 2008).

In addition to providing the k_a and k_d values, kinetic experiments conducted at different temperatures yield important insights into the molecular dynamics of complex formation. The energetic kinetic parameters (Eq. (4) – (7)) describing the formation of the activated complex (AC) can be calculated when the natural logarithms of the k_a and k_d values are plotted *versus* 1/T (the Arrhenius approach). The AC is an intermediate complex between free molecules and thermodynamically stable complexes. This complex is of short duration, is highly unstable, and can be present in several intermolecular interactions (Castro et al., 2021; McDonnell, 2001).

$$\mathrm{E_{act(y)}(T)} = -\mathrm{R}\left(\frac{\mathrm{d\ ln\ ln\ k(y)}}{\mathrm{dT}}\right) \tag{4}$$

$$k_y = \frac{k_B T}{h} exp - \left(\frac{\Delta G_y^{\ddagger}}{RT}\right) \tag{5}$$

$$\mathrm{\Delta H_y^{\ddagger}(T) = E_{ativ(y)}(T) - RT} \tag{6}$$

$$\mathrm{T\Delta S_y^{\ddagger}(T) = \Delta H_y^{\ddagger}(T) - \Delta G_y^{\ddagger}(T)} \tag{7}$$

where $E_{act\ (y)}^{\ddagger}$ is the activation energy required to form the activated complex. $\Delta G_y^{\ddagger}$ and $\Delta H_y^{\ddagger}$ are the activation Gibbs free energy and activation enthalpy changes, respectively, while $T\Delta S_y^{\ddagger}$ is the activation entropy change (for the formation of an activated complex by the association of free molecules (y = a) and dissociation of the

stable complex (y = d)). R is the universal gas constant (8.3145 J.mol^{-1}.K^{-1}), k_y is the association (k_a) or dissociation (k_d) constant (M^{-1}.s^{-1} and s^{-1}, respectively), k_B is the Boltzmann constant (1.38066 × 10^{-23} J.K^{-1}), and *h* is Planck's constant (6.62608 × 10^{-34} J.s) at temperature T (K).

According to the Arrhenius graph (Figure 3), the kinetic constants were influenced by temperature, demonstrating nonlinear relationships. This result suggests that the formation of AC, both by the association of free molecules and dissociation of the stable complex, occurred in multi-step processes (Allen et al., 1990), deriving from conformational fits in the binding site of βLG and the RES molecule. Conversely, the interaction of HSA with RES under similar temperature and pH conditions analyzed by Rezende et al. (2020) suggested that the potential energy barrier to form the activated complex was independent of temperature; therefore, the formation of the activated complex occurred in a single step. This discrepancy indicates that the protein structure influences complex formation.

Figure 3 - Arrhenius plots of ln k_a (■) and ln k_d (□) associated with βLG-RES interactions as functions of reciprocal temperature. Polynomial equation for the association process are as follows: $\ln k_a$ = - (7.52 x 10^2) + (4.50 x 10^5)T – (6.66 x 10^7)T^2 and R^2 = 0.952 (fitted model using F test, p-value < 0.05). Polynomial equation for the dissociation process are as follows: $\ln k_d$ = 58.71 - (3.30 x 10^4)T – (4.52 x 10^6)T^2 and R^2 = 0.999 (fitted model using F test, p-value < 0.05).

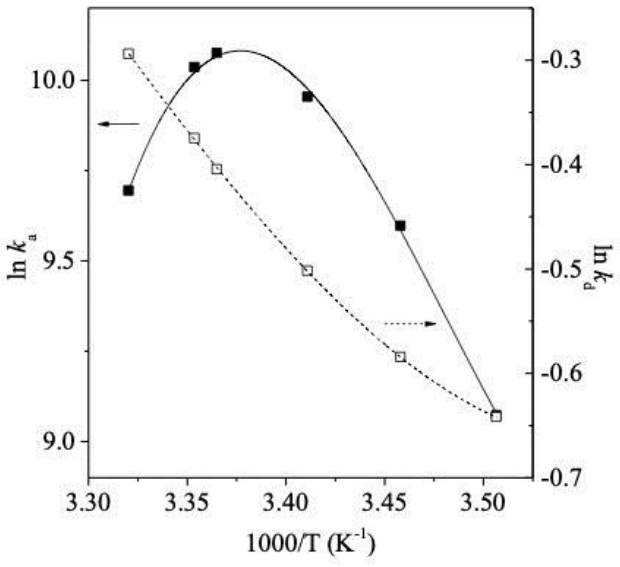

The kinetic energy parameters involved in the formation of the activated complex were also influenced by temperature (Figure 4). Therefore, through experimental data, we fitted mathematical models to the data to analyze the relationship between temperature (T) and the response of each parameter, as shown in Table 2.

Figure 4 - Energetic parameters for the formation of the activated complex between βLG and RES from the association of free molecules (■) or dissociation of the stable complex (□) at pH 7.4. (a) Activation energy required to form the activated complex ($E_{act(y)}$), (b) activation enthalpy change ($\Delta H_y^{\ddagger}$), (c) activation entropy change ($T\Delta S_y^{\ddagger}$), and (d) activation Gibbs free energy change ($\Delta G_y^{\ddagger}$). The black lines are the non-linear fitting, whose determination coefficients were greater than 0.999 in all cases.

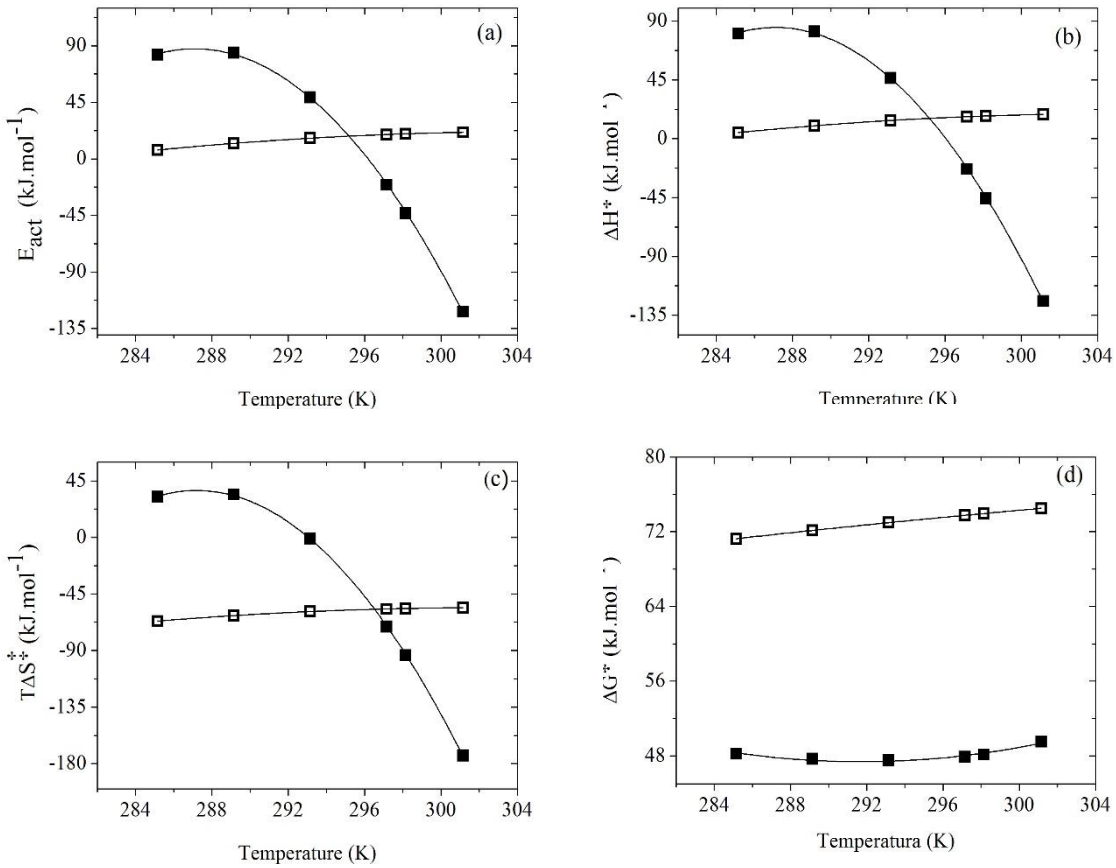

Table 2. Temperature relationship (T) in the response of kinetic parameters.

Parameter[1]	Equation[2]		R^2
$E^{\ddagger}_{act\ (y)}$	$E^{\ddagger}_{act\ (a)}$ = - (8.78 x 10^4) + (6.11 x 10^2)T – 1.07T^2	(8)	0.999
	$E^{\ddagger}_{act\ (d)}$= - (2.43 x 10^2) + 0.88T	(9)	0.958
$\Delta G^{\ddagger}_{y}$	$\Delta G^{\ddagger}_{a}$ = - (1.94 x 10^3) – 12.96T + 0.02T^2	(10)	0.927
	$\Delta G^{\ddagger}_{d}$ = 13.32 + 0.20T	(11)	0.999
$\Delta H^{\ddagger}_{y}$	$\Delta H^{\ddagger}_{a}$ = - (8.77 x 10^4) + (6.11 x 10^2)T – 1.06T^2	(12)	0.999
	$\Delta H^{\ddagger}_{d}$ = - (2.43 x 10^2) + 0.87T	(13)	0.958
$T\Delta S^{\ddagger}_{y}$	$T\Delta S^{\ddagger}_{a}$ = - (8.96 x 10^4) + (6.24 x 10^2)T – 1.09T^2	(14)	0.999
	$T\Delta S^{\ddagger}_{d}$ = - (2.57x 10^2) + 0.67T	(15)	0.935

[1](y = a) = association and (y = d) = dissociation. [2]Units are presented in KJ.mol^{-1}. Fitted model using the F-test, p-value < 0.05.

From the data of association of free molecules to form the AC in Fig. 4, we determined that the increase in temperature remarkably decreased $E^{\ddagger}_{act\ (a)}$ and $\Delta H^{\ddagger}_{a}$, from positive (82.86 and 80.49 kJ.mol^{-1}, respectively, at 285.15 K) to negative (-121.58 and -124.08 KJ.mol^{-1}, respectively, at 301.15 K) values.

For the temperatures studied initially (up to 296.17 K for $E^{\ddagger}_{act\ (a)}$ and 296.04 K for $\Delta H^{\ddagger}_{a}$), the positive values indicated the presence of an energy barrier in the formation of AC. Energy was absorbed at low temperatures to release the highly structured water molecules in the solvation layers of βLG and RES and change the conformation of the βLG binding site that presented low flexibility. Therefore, the potential rotational energy barrier present in the protein-binding site was greater compared with the kinetic energy resulting from collisions (KT) (Nunes et al., 2019). However, the values of $E^{\ddagger}_{act\ (a)}$ and $\Delta H^{\ddagger}_{a}$ became negative from 296.17 and 296.04 K. This can be explained by the fact that the water molecules in the solvation layers became less structured with an increase in the system temperature; hence, the structural or energy difference between the solvation layers and the water molecules present in the bulk was reduced (Hudson et al., 2022). Additionally, the protein-binding site became more flexible because of the increase in the molecular collisional energy (3/2 KT). The decrease in the structural or energy difference and the increase

in the protein-binding site flexibility reduce the energy required for releasing water molecules from the solvation layers and fitting the protein-binding site. Thus, the energy released from the βLG-RES intermolecular interaction (E_{int}) overcomes the energy of desolvation (E_{dess}) and conformational change (E_{conf}): $|E_{int}| > |E_{conf} + E_{dess}|$.

The values of $E^{\ddagger}_{act\,(d)}$ and $\Delta H^{\ddagger}_{d}$ were positive (< 21.15 and 18.65 kJ.mol^{-1}, respectively) and almost unchanged throughout all the studied temperatures (slope of linear fitting (α) equal to 0.88 and 0.87, respectively). This observation was attributed to the conformation of the stable thermodynamic complex in βLG-RES interaction, which was almost analogous to that of AC. The obtained result was also different compared to the HSA-RES interaction, wherein the values of $E^{\ddagger}_{act\,(d)}$ and $\Delta H^{\ddagger}_{d}$ were -3.06 kJ.mol^{-1} and -5 kJ.mol^{-1}, respectively. Because RES interacts with the hydrophobic cavity of βLG (Cheng et al., 2018), the water content in the protein-binding site does not change in AC and the thermodynamically stable complex. Therefore, conformational change is the main energy contributor to obtaining an AC from a thermodynamically stable complex.

The entropic term for the association of free molecules to form AC exhibited polynomial behavior (Fig. 4c and Table 2). The $T\Delta S^{\ddagger}_{a}$ values were positive until 289.15 K, subsequently becoming negative. The same reasoning as discussed for $\Delta H^{\ddagger}_{a}$ values can be applied here. The $T\Delta S^{\ddagger}_{a}$ values are the sums of the three terms (Eq. (16)) (Paiva et al., 2020):

$$T\Delta S^{\circ} = \Delta S^{\circ}_{des} + \Delta S^{\circ}_{conf} + \Delta S^{\circ}_{int} \qquad (16)$$

where ΔS°_{des} is the standard entropy change that is associated with solvent release during the binding of βLG and RES, ΔS°_{conf} is the entropy change that is associated with the conformational change of the βLG binding site, and ΔS°_{int} is the standard entropy change related to the βLG-RES interaction.

As previously discussed, the βLG binding site is in the lowest energetic and highest structural states at low temperatures (T < 289.15 K). When the βLG-RES complex is formed, the βLG-binding site fitting process destructures the βLG site, increasing conformational entropy. In addition, the release of more structured water molecules from the solvation layer of interacting molecules at low temperatures increases the configurational entropy (S_{conf}) of the system because the released

water molecules have a great degree of translational freedom. Conversely, the βLG binding site became more flexible at temperatures above 289.15 K (that is, the ΔS°_{conf} contribution reduced). Additionally, the difference between the degrees of freedom of water molecules in the solvation layer and bulk at a higher temperature also reduced, decreasing the contribution of ΔS°_{des}. Hence, the ΔS°_{int} prevailed owing to the direct interaction between βLG and RES, resulting in negative $T\Delta S^{\ddagger}_{a}$ values.

In contrast to $T\Delta S^{\ddagger}_{a}$, the $T\Delta S^{\ddagger}_{d}$ values were negative at all temperatures. This result indicates structuration of the binding site of βLG to form AC from a thermodynamically stable complex. Hence, independent of temperature, the amino acid residues in the AC are more orientated around the RES molecule compared to that in the thermodynamically stable complex.

The $\Delta G^{\ddagger}_{y}$ values were almost constant at all studied temperatures. However, the $\Delta G^{\ddagger}_{d}$ values were approximately 1.5 times greater than the $\Delta G^{\ddagger}_{a}$ values, mainly because of the absence of energetic parameters associated with the structural changes in the solvation layers of βLG-RES complexes. This greater energetic barrier in the dissociation process arises from the structuration increase of amino acid residues around the RES molecule, which occurs during the transition from the thermodynamically stable complex to AC. This greater structuring of amino acids rapidly forms AC from the association of free molecules compared to that from the dissociation of the thermodynamically stable βLG-RES complex.

The almost unchanged $\Delta G^{\ddagger}_{y}$ values with increasing temperature suggest the occurrence of isokinetic compensation (IKC) between $\Delta H^{\ddagger}_{y}$ and $T\Delta S^{\ddagger}_{y}$, that is, $\Delta H^{\ddagger}_{y}$ and $T\Delta S^{\ddagger}_{y}$ increase at the same rate. To prove the IKC hypothesis, we plotted a graph of $T\Delta S^{\ddagger}_{y}$ *versus* $\Delta H^{\ddagger}_{y}$ (Fig. 3S). We confirmed the compensatory effect from the slope of the linear fitting (α) close to 1 (α_a = 1.01, $R^2_{(a)}$ = 0.999, and α_d = 0.77, $R^2_{(d)}$ = 0.997. Isokinetic compensation indicates the optimization of the system energy to form AC (Garvín et al., 2017), which can be associated with desolvation and the conformational change at the βLG interaction site in the association step and conformation fitting of the protein in the dissociation step (Felix et al., 2019).

Supplementary Figure S3 - Isokinetic compensation graph (IKC) for the formation of the activated complex between βLG and RES from the association of free molecules (■) or dissociation of the stable complex (□) at pH 7.4.

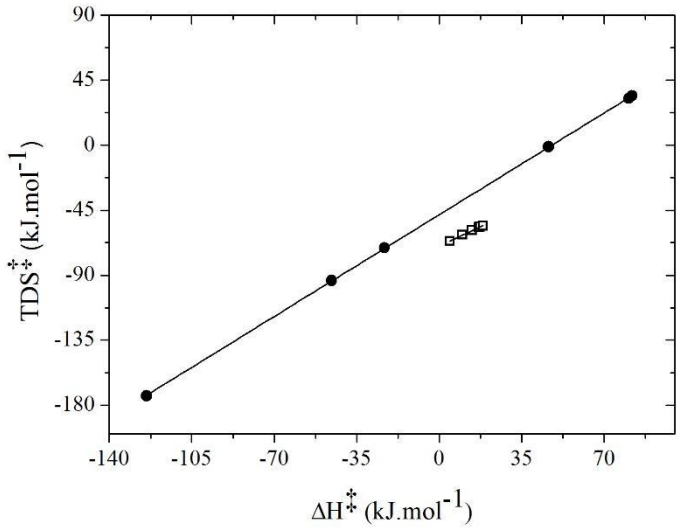

Finally, to evaluate the intensity of the interactions occurring before and after AC formation, the activation specific heat change ($\Delta C_{p\,(y)}^{\ddagger}$) was calculated using Eq. (17).

$$\left(\frac{\partial H_{(y)}^{\ddagger}}{\partial T}\right)_{P} = \Delta C_{p\,(y)}^{\ddagger} \qquad (17)$$

The value of $\Delta C_{p\,(a)}^{\ddagger}$ corresponds to the difference between the C_P of the activated complex ($C_{P,\beta LG-RES}^{\ddagger}$) and the sum of the C_P of the free molecules ($C_{P,\beta LG} + C_{P,RES,}$). Similarly, $\Delta C_{p\,(d)}^{\ddagger}$ corresponds to the difference between $C_{P,\beta LG-RES}$ and C_P of the stable complex ($C_{P,stable\ \beta LG-RES,}$) (Nunes et al., 2019).

The values obtained for $\Delta C_{p\,(a)}^{\ddagger}$ and for $\Delta C_{p\,(d)}^{\ddagger}$ are illustrated in Table 3.

Table 3. Change of specific heat of activation for association ($\Delta C_{p\,(a)}^{\ddagger}$) and dissociation ($\Delta C_{p\,(d)}^{\ddagger}$).

T (K)	$\Delta \boldsymbol{C}_{\boldsymbol{p}\,(\boldsymbol{a})}^{\ddagger}$	$\Delta \boldsymbol{C}_{\boldsymbol{p}\,(\boldsymbol{d})}^{\ddagger}$
	kJ.K^{-1}.mol^{-1}	
285.15	4.15	1.46
289.15	-4.37	1.16
293.15	-12.89	0.87
297.15	-21.40	0.58
298.15	-23.53	0.51
301.15	-29.92	0.29

The $\Delta C_{p\,(a)}^{\ddagger}$ was positive at 285.15 K and negative at all other temperatures, that is, the positive contribution for $\Delta C_{p\,(a)}^{\ddagger}$from the conformational change and the direct βLG-RES interaction overcame the negative desolvation effect at the lowest temperature. However, at high temperatures, the release of solvation water molecules prevailed over the new interactions formed by complex synthesis. As discussed above, the βLG-binding site was less flexible at low temperatures; therefore, a greater orientation of amino acid residues around the RES molecule was observed, increasing the strength of interactions occurring in the AC stronger compared to those prevailing when βLG and RES were free in solution. Conversely, the binding site in the protein became more flexible with an increase in temperature, with sufficient energy to allow the free rotation of the amino acid residues. Hence, the intensity of hydrogen bonds is reduced, which decreased the potential energy stored in the bonds and results in $C_{P,\beta LG-RES}^{\ddagger} < C_{P,\beta LG} + C_{P,RES}$.

The $\Delta C_{p\,(d)}^{\ddagger}$ values were positive at all temperature ranges and were smaller than those obtained for $\Delta C_{p\,(a)}^{\ddagger}$ (in modulus). The low $\Delta C_{p\,(d)}^{\ddagger}$ values demonstrated the interactions of AC and thermodynamically stable complexes with similar magnitudes. In addition, the $\Delta C_{p\,(d)}^{\ddagger}$ values decreased as the temperature increased, indicating that the orientation of amino acid residues around the RES molecule was reduced at higher temperatures, which decreased the intensity of RES-amino acid interactions.

The dependence of $\Delta C^{\ddagger}_{p\,(d)}$ on temperature corroborates our interpretation of the results obtained for $T\Delta S^{\ddagger}_{d}$ values.

3.3 Thermodynamics of the RES interaction with immobilized βLG

Additionally, SPR allowed us to determine the thermodynamics of the complex formation. It is important to understand the stability of the βLG-RES complex and to assess the driving forces in the complex formation.

The binding constant (K_b) was calculated using the relationship between k_a and k_d ($K_b = k_a/k_d$). The K_b temperature dependence was analyzed using a nonlinear van't Hoff approach (ln K_b *versus* 1/T); a polynomial model (ln K_b= $a + b\left(\frac{1}{T}\right) + c\left(\frac{1}{T}\right)^2 + d\left(\frac{1}{T}\right)^3$) was fitted to the van't Hoff data. The standard Gibbs free energy change ($\Delta G°$), enthalpy change ($\Delta H°$), and entropy change ($T\Delta S°$) of the complex formation were calculated using Eq. (17) – (19).

$$\Delta G° = -RTlnK_b \tag{17}$$

$$\Delta H° = -R\frac{\partial(ln\ K_b)}{\partial(\frac{1}{T})} \tag{18}$$

$$T\Delta S° = \Delta H° - \Delta G° \tag{19}$$

where R is the universal gas constant (8.3145 J.mol^{-1}.K^{-1}), T is the temperature (K), and a, b, c, d, and ln φ are constants graphically determined by the polynomial adjustment of the van't Hoff nonlinear approach.

The values obtained for K_b ranged from 1.65 to 3.55 × 10^4 L.mol^{-1}; the formation of βLG-RES complex was greater at 294.47 K (Figure 5).

Figure 5 - Binding constants for the βLG-RES interaction.

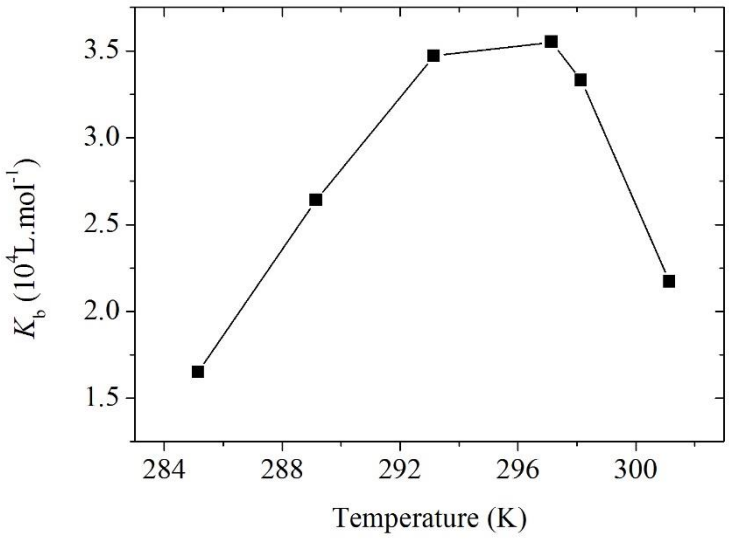

The value of K_b determined by Guo and Jauregi (2018) was 4.8 times greater than that in our present study (K_bβLG-*trans*RES = 1.67 x 10^5 M^{-1}) at 293 K and pH 7.4. The differences between the results can be attributed to the different experimental techniques used. Guo and Jauregi used FS, wherein βLG and RES were in the solution. Conversely, in the present SPR technique, the protein is immobilized over a chip, which restricts the degree of translational freedom of the macromolecule and consequently the entropic contribution to complex formation. Thus, it is essential to study this condition of immobilized proteins because proteins are adsorbed on interfaces in several food systems, which also limits their degree of translational freedom (Felix et al., 2019).

The thermodynamic parameters and mathematical fitting results obtained for βLG-RES complex formation are shown in Figure 6 Table 1S, respectively.

Figure 6 - Thermodynamic parameters for the formation of the stable complex between βLG and RES at pH 7.4. (Δ) $\Delta G°$, $\Delta H°$ (▪), and T$\Delta S°$ (○).

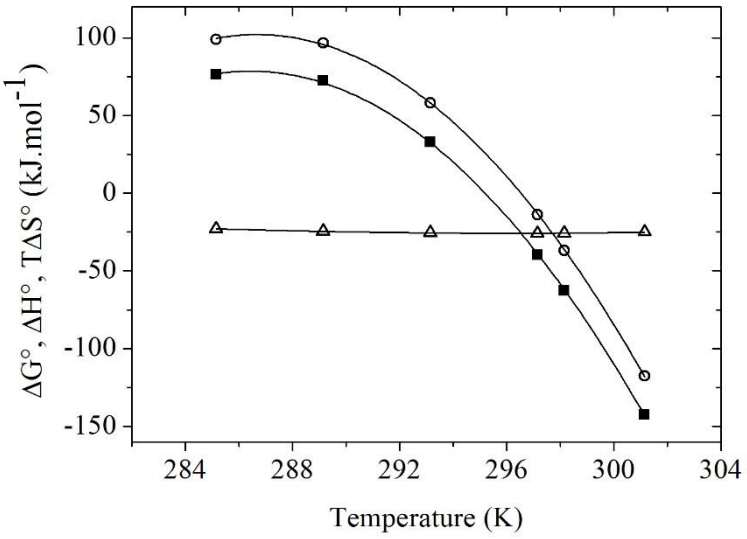

Supplementary Table 1

Relationship between temperature (T) and the response of thermodynamic parameters.

Parameter	Equation*		R^2
$\Delta G°$	$\Delta G° = (2.05 \times 10^3) - 14.01T - 0.02T^2$	(20)	0.970
$\Delta H°$	$\Delta H° = (8.43 \times 10^4) - (5.89 \times 10^2)T - 1.03T^2$	(21)	0.999
T$\Delta S°$	$T\Delta S° = (8.63 \times 10^4) - (6.03 \times 10^2)T + 1.05T^2$	(22)	0.999

*Units are presented in KJ.mol^{-1}. Fitted model using the F-test, p-value < 0.05.

The negative $\Delta G°$ values (-24.95 KJ.mol^{-1}) indicated more formation of complexes over free molecules. Compared to HSA-RES interaction (-18.94 KJ.mol^{-1}), βLG-RES is more stable; hence, the RES molecules are primarily carried by βLG at the same protein and RES concentrations.

For a better understanding on the mechanism of βLG-RES complex formation, we addressed the components of $\Delta G°$. As shown in Eq. (19), ΔG° present the enthalpic and entropic contributions. $\Delta H°$ and the $T\Delta S°$ demonstrated similar descendant second-order polynomial behavior, which was positive up to 295.2 K and 296.5 K, respectively.

As discussed previously for AC formation, the $\Delta H°$ values result from the enthalpies of desolvation, conformational change, and interaction ($\Delta H°_{dess}$, $\Delta H°_{conf,}$ and $\Delta H°_{int}$, respectively), as shown in Eq. (23).

$$\Delta H° = \Delta H°_{des} + \Delta H°_{conf} + \Delta H°_{int} \quad (23)$$

Between 285.15 and 295.2 K, the ΔH° values were positive because $\Delta H°_{des}$ and $\Delta H°_{conf}$ were positive and greater than the $\Delta H°_{int}$ modulus ($\Delta H°_{int} < 0$). The energy absorbed to break the H_2O-βLG and H_2O-RES interactions was higher than that released during H_2O-H_2O H bond formed in the bulk of the system. This positive energy result occurred because the water molecules in the solvation layers were more oriented compared to those in bulk, promoting strong H bonds. In addition, the low temperature decreased the flexibility of the protein-binding site, increasing the energy required to change the conformation of the βLG interaction site. In contrast, the difference in the 3D structure of water molecules in the solvation layers of interacting molecules and in bulk decreases at high temperatures, reducing $\Delta H°_{des}$. Additionally, the high temperature increased the flexibility of the βLG binding site, decreasing the $\Delta H°_{conf}$ contribution. Hence, the ΔH° values became negative at T > 297.15 K.

When analyzing the entropic contribution (Eq. (24)), we must consider that the TΔS° values are acquired from the changes in the conformational entropy ($T\Delta S_{conf}$) and configurational entropy ($T\Delta S_{config}$). The $T\Delta S_{config}$can be divided into $\Delta S_{config-W}$ owing to the release of water molecules from the solvation layer ($T\Delta S_{config-W} > 0$) and $T\Delta S_{config-int}$ because of the direct βLG-RES interaction ($T\Delta S_{config-int} < 0$).

$$T\Delta S° = T\Delta S_{conf} + T\Delta S_{config-W} + T\Delta S_{config-int} \quad (24)$$

As discussed previously ΔH° values, the TΔS° values were positive at a temperature below 296.5 K, ranging from 99.06 to 58.16 KJ.mol^{-1}. The positive values are attributed $T\Delta S_{conf}$ and $T\Delta S_{config-W}$, which are positive and overcome negative $T\Delta S_{config-int}$. Conversely, at T > 296.5 K, $T\Delta S_{config-int}$ prevailed over $T\Delta S_{conf}$ and $T\Delta S_{config-W}$, resulting in negative TΔS° values.

As discussed previously in AC formation, the almost unchanged ΔG° values and linear relationship between ΔH° and TΔS° (α = 0.99, R^2 = 0.999; Figure 4S) indicated a compensation between enthalpy and entropy components, that is, the enthalpy-

entropy compensation (EEC). This EEC indicates that the system optimized energy to form the βLG-RES complex based on the desolvation process and conformational change of the protein. As the temperature increased, the decrease in the ΔH° values was compensated by the simultaneous (and of a similar magnitude) decrease of TΔS° values.

Supplementary Figure S4 - Enthalpy-entropy compensation (EEC) for the formation of the stable complex βLG-RES.

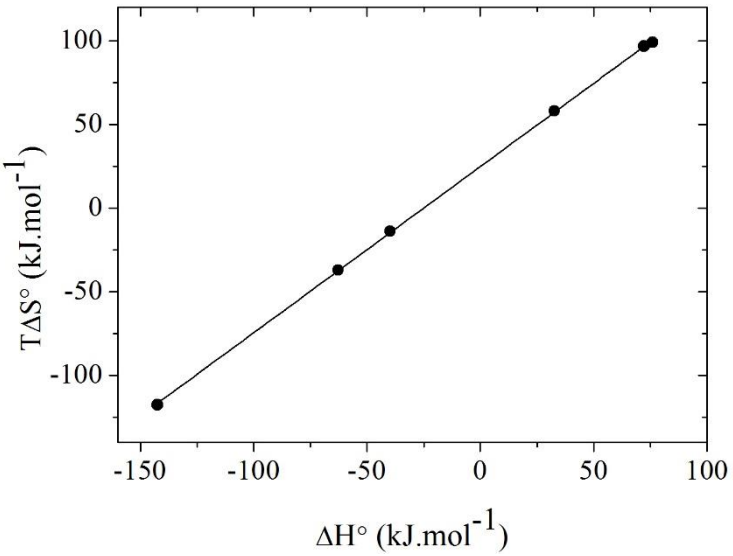

4 . Conclusions

The association process between free βLG and RES molecules is dependent on the degree of water structuration on the solvation shell of both molecules. The energetic cost for releasing water molecules from the solvation shell to the bulk determine the values of all association kinetic parameters ($E^{\ddagger}_{act\,(a)}$, $\Delta H^{\ddagger}_{a}$, $T\Delta S^{\ddagger}_{a}$, $\Delta G^{\ddagger}_{y}$, and $\Delta C^{\ddagger}_{p\,(a)}$). The solvation water modulation of βLG-RES interaction occurs via a compensation process between $\Delta H^{\ddagger}_{a}$ and $T\Delta S^{\ddagger}_{a}$ (isokinetic compensation). On the other hand, the dissociation process of the βLG-RES thermodynamic stable complex is not dependent on the solvation shell of βLG and RES complex molecules. This dissociation behavior shows that the water concentration around the βLG-RES interaction site should be lower and the few water presents are not structured.

The βLG-RES nanocomplex formation was promoted by hydrophobic interaction when the temperature was lower, while hydrophilic forces drove the βLG-RES interaction at a higher temperature. This thermodynamic and kinetic knowledge about βLG and RES interaction makes it possible to modulate, by changing the thermodynamic state of the system, the carrier, and release of RES by βLG.

Acknowledgments

The authors thank the Coordenação de Aperfeiçoamento de Pessoal de Nível Superior (CAPES), CAPES/Pró-Forenses, Conselho Nacional de Desenvolvimento Científico e Tecnológico (CNPq), Fundação de Apoio à Pesquisa de Minas Gerais (FAPEMIG), and Financiadora de Estudos e Projetos (FINEP), for their financial support.

5 . References

Dima, I. G., Aprodu, I., Râpeanu, G., & Stănciuc, N. (2018). Binding mechanisms between lycopene extracted from tomato peels and bovine β-lactoglobulin. *Journal of Luminescence*, *203*(April), 582–589. https://doi.org/10.1016/j.jlumin.2018.07.017

Allen, B., Blum, M., Cunningham, A., Tu, G.-C., & Hofmann, T. (1990). A Ligand-induced , Change in Penicillopepsin. *The Journal of Biological Chemistry*, *265*(9), 5060–5065.

Arcanjo, N. M. O., Luna, C., Madruga, M. S., & Estévez, M. (2018). Antioxidant and pro-oxidant actions of resveratrol on human serum albumin in the presence of toxic diabetes metabolites: Glyoxal and methyl-glyoxal. *Biochimica et Biophysica Acta (BBA) - General Subjects*, *1862*(9), 1938–1947. https://doi.org/10.1016/j.bbagen.2018.06.007

Bourassa, P., Kanakis, C. D., Tarantilis, P., Pollissiou, M. G., & Tajmir-Riahi, H. A. (2010). Resveratrol, genistein, and curcumin bind bovine serum albumin. *Journal of Physical Chemistry B*, *114*(9), 3348–3354. https://doi.org/10.1021/JP9115996/asset/images/medium/jp-2009-115996_0008.GIF

Castro, A. S. B., de Paula, H. M. C., Coelho, Y. L., Hudson, E. A., Pires, A. C. S., &

da Silva, L. H. M. (2021). Kinetic and thermodynamic of lactoferrin – Ethoxylated-nonionic surfactants supramolecular complex formation. *International Journal of Biological Macromolecules*, *187*, 325–331. https://doi.org/10.1016/j.ijbiomac.2021.07.087

Cao, S., Wang, D., Tan, X., & Chen, J. (2009). Interaction Between Trans-resveratrol and Serum Albumin in Aqueous Solution. *Journal of Solution Chemistry 2009 38:9*, *38*(9), 1193–1202. https://doi.org/10.1007/S10953-009-9439-7

Chen, J. Y., Zhu, Q., Zhang, S., OuYang, D., & Lu, J. H. (2019). Resveratrol in experimental Alzheimer's disease models: A systematic review of preclinical studies. *Pharmacological Research*, *150*(August), 104476. https://doi.org/10.1016/j.phrs.2019.104476

Cheng, H., Dong, H., Wusigale, & Liang, L. (2020). A comparison of β-casein complexes and micelles as vehicles for trans-/cis-resveratrol. *Food Chemistry*, *330*, 127209. https://doi.org/10.1016/j.foodchem.2020.127209

Cheng, H., Fang, Z., Wusigale, Bakry, A. M., Chen, Y., & Liang, L. (2018). Complexation of trans- and cis-resveratrol with bovine serum albumin, β-lactoglobulin or α-lactalbumin. *Food Hydrocolloids*, *81*, 242–252. https://doi.org/10.1016/j.foodhyd.2018.02.037

Coelho, Y. L., de Paula, H. M. C., Agudelo, A. J. P., de Castro, A. S. B., Hudson, E. A., Pires, A. C. S., & Silva, L. H. M. (2019). Lactoferrin-phenothiazine dye interactions: Thermodynamic and kinetic approach. *International Journal of Biological Macromolecules*, *136*, 559–569. https://doi.org/10.1016/j.ijbiomac.2019.06.097

Dai, T., Li, R., Liu, C., Liu, W., Li, T., Chen, J., Kharat, M., & McClements, D. J. (2019). Effect of rice glutelin-resveratrol interactions on the formation and stability of emulsions: A multiphotonic spectroscopy and molecular docking study. *Food Hydrocolloids*, *97*, 105234. https://doi.org/10.1016/j.foodhyd.2019.105234

Fan, Y., Liu, Y., Gao, L., Zhang, Y., & Yi, J. (2018). Improved chemical stability and cellular antioxidant activity of resveratrol in zein nanoparticle with bovine serum albumin-caffeic acid conjugate. *Food Chemistry*, *261*, 283–291. https://doi.org/10.1016/j.foodchem.2018.04.055

Felix, M., Yang, J., Guerrero, A., & Sagis, L. M. C. (2019). Effect of cinnamaldehyde on interfacial rheological properties of proteins adsorbed at O/W interfaces. *Food*

Hydrocolloids, *97*, 105235. https://doi.org/10.1016/j.foodhyd.2019.105235

Garvín, A., Ibarz, R., & Ibarz, A. (2017). Kinetic and thermodynamic compensation. A current and practical review for foods. *Food Research International*, *96*, 132–153. https://doi.org/10.1016/j.foodres.2017.03.004

Guo, Y., & Jauregi, P. (2018). Protective effect of β-lactoglobulin against heat induced loss of antioxidant activity of resveratrol. *Food Chemistry*, *266*, 101–109. https://doi.org/10.1016/j.foodchem.2018.05.108

Hudson, E., Campos de Paula, H. M., Coelho, Y. L., Glanzmann, N., da Silva, A. D., Mendes da Silva, L. H., & dos Santos Pires, A. C. (2022). The kinetics of formation of resveratrol-β-cyclodextrin-NH2 and resveratrol analog-β-cyclodextrin-NH2 supramolecular complexes. *Food Chemistry*, *366*, 130612. https://doi.org/10.1016/j.foodchem.2021.130612

Jiang, Y. L. (2008). Design, synthesis and spectroscopic studies of resveratrol aliphatic acid ligands of human serum albumin. *Bioorganic & Medicinal Chemistry*, *16*(12), 6406–6414. https://doi.org/10.1016/j.bmc.2008.05.002

Kotta, S., Mubarak Aldawsari, H., Badr-Eldin, S. M., Alhakamy, N. A., & Md, S. (2021). Coconut oil-based resveratrol nanoemulsion: Optimization using response surface methodology, stability assessment and pharmacokinetic evaluation. *Food Chemistry*, *357*, 129721. https://doi.org/10.1016/j.foodchem.2021.129721

Liang, L., & Subirade, M. (2012). Study of the acid and thermal stability of β-lactoglobulin–ligand complexes using fluorescence quenching. *Food Chemistry*, *132*(4), 2023–2029. https://doi.org/10.1016/j.foodchem.2011.12.043

Liang, L., Tajmir-Riahi, H. A., & Subirade, M. (2008). Interaction of β-Lactoglobulin with resveratrol and its biological implications. *Biomacromolecules*, *9*(1), 50–56. https://doi.org/10.1021/bm700728K

Liang, Q., Ren, X., Zhang, X., Hou, T., Chalamaiah, M., Ma, H., & Xu, B. (2018). Effect of ultrasound on the preparation of resveratrol-loaded zein particles. *Journal of Food Engineering*, *221*, 88–94. https://doi.org/10.1016/j.jfoodeng.2017.10.002

Liu, Q., Qin, Y., Jiang, B., Chen, J., & Zhang, T. (2022). Development of self-assembled zein-fucoidan complex nanoparticles as a delivery system for resveratrol. *Colloids and Surfaces B: Biointerfaces*, *216*, 112529. https://doi.org/10.1016/j.colsurfb.2022.112529

Lu, Z., Zhang, Y., Liu, H., Yuan, J., Zheng, Z., & Zou, G. (2007). Transport of a Cancer Chemopreventive Polyphenol, Resveratrol: Interaction with Serum Albumin and Hemoglobin. *Journal of Fluorescence 2007 17:5*, *17*(5), 580–587. https://doi.org/10.1007/S10895-007-0220-2

McDonnell, J. M. (2001). Surface plasmon resonance: towards an understanding of the mechanisms of biological molecular recognition. *Current Opinion in Chemical Biology*, *5*(5), 572–577. https://doi.org/10.1016/S1367-5931(00)00251-9

N′ soukpoé-Kossi, C. N., St-Louis, C., Beauregard, M., Subirade, M., Carpentier, R., Hotchandani, S., & Tajmir-Riahi, H. A. (2006). Resveratrol binding to human serum albumin. *Journal of Biomolecular Structure & Dynamics*, *24*(3), 277–283. https://doi.org/10.1080/07391102.2006.10507120

Nair, M. S. (2015). Spectroscopic study on the interaction of resveratrol and pterostilbene with human serum albumin. *Journal of Photochemistry and Photobiology B: Biology*, *149*, 58–67. https://doi.org/10.1016/j.jphotobiol.2015.05.001

Nguyen, H. H., Park, J., Kang, S., & Kim, M. (2015). Surface Plasmon Resonance: A Versatile Technique for Biosensor Applications. *Sensors (Basel, Switzerland)*, *15*(5), 10481. https://doi.org/10.3390/S150510481

Nunes, N. M., de Paula, H. M. C., Coelho, Y. L., da Silva, L. H. M., & Pires, A. C. S. (2019). Surface plasmon resonance study of interaction between lactoferrin and naringin. *Food Chemistry*, *297*, 125022. https://doi.org/10.1016/j.foodchem.2019.125022

Paiva, P. H. C., Coelho, Y. L., da Silva, L. H. M., Pinto, M. S., Vidigal, M. C. T. R., & Pires, A. C. dos S. (2020). Influence of protein conformation and selected Hofmeister salts on bovine serum albumin/lutein complex formation. *Food Chemistry*, *305*, 125463. https://doi.org/10.1016/j.foodchem.2019.125463

Pantusa, M., Sportelli, L., & Bartucci, R. (2012). Influence of stearic acids on resveratrol-HSA interaction. *European Biophysics Journal 2012 41:11*, *41*(11), 969–977. https://doi.org/10.1007/S00249-012-0856-Y

Poór, M., Kaci, H., Bodnárová, S., Mohos, V., Fliszár-Nyúl, E., Kunsági-Máté, S., Özvegy-Laczka, C., & Lemli, B. (2022). Interactions of resveratrol and its metabolites (resveratrol-3-sulfate, resveratrol-3-glucuronide, and dihydroresveratrol) with serum albumin, cytochrome P450 enzymes, and OATP transporters. *Biomedicine & Pharmacotherapy*, *151*, 113136.

https://doi.org/10.1016/j.biopha.2022.113136

Pujara, N., Jambhrunkar, S., Wong, K. Y., McGuckin, M., & Popat, A. (2017). Enhanced colloidal stability, solubility and rapid dissolution of resveratrol by nanocomplexation with soy protein isolate. *Journal of Colloid and Interface Science*, *488*, 303–308. https://doi.org/10.1016/j.jcis.2016.11.015

Rezende, J. de P., De Paula, H. M. C., Freitas, T. D., Coelho, Y. L., Da Silva, L. H. M., & Pires, A. C. dos S. (2022). Application of Congo red dye as a molecular probe to investigate the kinetics and thermodynamics of the formation processes of arachin and conarachin nanocomplexes. *Food Chemistry*, *384*, 132485. https://doi.org/10.1016/j.foodchem.2022.132485

Rezende, J. de P., Hudson, E. A., De Paula, H. M. C., Meinel, R. S., Da Silva, A. D., Da Silva, L. H. M., & Pires, A. C. dos S. (2020). Human serum albumin-resveratrol complex formation: Effect of the phenolic chemical structure on the kinetic and thermodynamic parameters of the interactions. *Food Chemistry*, *307*, 125514. https://doi.org/10.1016/j.foodchem.2019.125514

Robertson, I., Wai Hau, T., Sami, F., Sajid Ali, M., Badgujar, V., Murtuja, S., Saquib Hasnain, M., Khan, A., Majeed, S., & Tahir Ansari, M. (2022). The science of resveratrol, formulation, pharmacokinetic barriers and its chemotherapeutic potential. *International Journal of Pharmaceutics*, 121605. https://doi.org/10.1016/j.ijpharm.2022.121605

Su, Y. W., Fang, Y. M., & Li, T. F. (2021). Surface plasmon resonance sensing in cell biology and drug discovery. *Comprehensive Analytical Chemistry*, *95*, 1–53. https://doi.org/10.1016/bs.coac.2021.06.004

Vijayalakshmi, L., Krishna, R., Sankaranarayanan, R., & Vijayan, M. (2008). An asymmetric dimer of beta-lactoglobulin in a low humidity crystal form--structural changes that accompany partial dehydration and protein action. *Proteins*, *71*(1), 241–249. https://doi.org/10.1002/prot.21695

Wolf, F. A., & Brett, G. M. (2000). *Ligand-Binding Proteins: Their Potential for Application in Systems for Controlled Delivery and Uptake of Ligands*. http://www.pharmrev.org

Wusigale, Fang, Z., Hu, L., Gao, Y., Li, J., & Liang, L. (2017). Protection of resveratrol against the photodecomposition of folic acid and photodecomposition-induced structural change of beta-lactoglobulin. *Food Research International*, *102*, 435–444.

https://doi.org/10.1016/j.foodres.2017.09.006

Xu, Y., Wu, J., & Wang, S. (2021). Comparative study of whey protein isolate and gelatin treated by pH-shifting combined with ultrasonication in loading resveratrol. *Food Hydrocolloids*, *117*, 106694. https://doi.org/10.1016/j.foodhyd.2021.106694

Yi, J., He, Q., Peng, G., & Fan, Y. (2022). Improved water solubility, chemical stability, antioxidant and anticancer activity of resveratrol via nanoencapsulation with pea protein nanofibrils. *Food Chemistry*, *377*, 131942. https://doi.org/10.1016/j.foodchem.2021.131942

Zhang, J., Liu, X., Subirade, M., Zhou, P., & Liang, L. (2014). A study of multi-ligand beta-lactoglobulin complex formation. *Food Chemistry*, *165*, 256–261. https://doi.org/10.1016/j.foodchem.2014.05.109

Zhang, X., Lu, Y., Zhao, R., Wang, C., Wang, C., & Zhang, T. (2022). Study on simultaneous binding of resveratrol and curcumin to β-lactoglobulin: Multi-spectroscopic, molecular docking and molecular dynamics simulation approaches. *Food Hydrocolloids*, *124*, 107331. https://doi.org/10.1016/j.foodhyd.2021.107331

CONCLUSÕES GERAIS

Pelo presente estudo e utilizando a ressonância plasmônica de superfície (SPR), a dinâmica de interação entre βLG e o RES tornaram-se conhecidas. Os dados cinéticos e termodinâmicos proporcionaram o entendimento de como ocorre a formação de complexo βLG-RES. A associação das moléculas livres é mais rápida que a dissociação dos complexos termodinamicamente estáveis. Os parâmetros cinéticos de associação ($E^{\ddagger}_{act\,(a)}$, $\Delta H^{\ddagger}_{a}$, $T\Delta S^{\ddagger}_{a}$, $\Delta G^{\ddagger}_{y}$, e $\Delta C^{\ddagger}_{p\,(a)}$) são dependentes da estrutura 3D da água presente na camada de solvatação de ambas as moléculas. Por outro lado, os parâmetros cinéticos de dissociação, não foram dependentes da estrutura 3D da água que solvatam o complexo βLG-RES. Provavelmente, estas moléculas de água que interagem com o complexo não estão concentradas ao redor/dentro do sítio de interação da proteína. A mudança de temperatura interfere na formação de nanocomplexo βLG-RES. Em baixa temperatura, a formação de complexo é impulsionada pela interação hidrofóbica enquanto que em alta temperatura, as interações hidrofílicas são dominantes.

O conhecimento da dinâmica de interação entre βLG-RES permite o planejamento das melhores condições termodinâmicas para a formação e, aplicação destes nanocomplexos em diferentes áreas. Assim, nosso estudo abre precedente para outros que pretendem utilizar este tipo de molécula proteica para por exemplo, carrear o RES.